

MAY 13 1947

ARR Sept. 1942

NATIONAL ADVISORY COMMITTEE FOR AERONAUTICS

WARTIME REPORT

ORIGINALLY ISSUED

September 1942 as
Advance Restricted Report

WIND-TUNNEL TESTS OF SINGLE- AND DUAL-ROTATING TRACTOR PROPELLERS OF LARGE BLADE WIDTH

By David Biermann, W. H. Gray, and Julian D. Maynard

Langley Memorial Aeronautical Laboratory
Langley Field, Va.

1x5 - Item 8 . AF 1946

NACA

WASHINGTON

NACA WARTIME REPORTS are reprints of papers originally issued to provide rapid distribution of advance research results to an authorized group requiring them for the war effort. They were previously held under a security status but are now unclassified. Some of these reports were not technically edited. All have been reproduced without change in order to expedite general distribution.

L - 385

NACA LIBRARY
LANGLEY MEMORIAL AERONAUTICAL
LABORATORY
Langley Field, Va.

NATIONAL ADVISORY COMMITTEE FOR AERONAUTICS

ADVANCE RESTRICTED REPORT

WIND-TUNNEL TESTS OF SINGLE- AND DUAL-ROTATING

TRACTOR PROPELLERS OF LARGE BLADE WIDTH

By David Biermann, W. H. Gray, and Julian D. Maynard

SUMMARY

Tests of 10-foot diameter, single- and dual-rotating tractor propellers having from two to eight blades were conducted in the NACA 20-foot propeller-research tunnel of the Langley Memorial Aeronautical Laboratory. This work was a continuation of previous investigations of tractor propellers. The test program differed from the previous investigations only in the respect that the blades used were 50 percent wider than those previously employed. The propellers were mounted at the front end of a streamline body with a symmetrical wing in the slipstream.

The decrease of peak efficiency with increased solidity was very low. Increasing the solidity four times decreased the maximum efficiency by only 6 percent for single rotation. The percentage change was even less for dual rotation.

The effects of dual rotation and changes in solidity were, in general, the same as the effects found in previous investigations of standard blades.

INTRODUCTION

Recent increases in airplane engine power and in the altitude of flight have made it necessary to provide propellers of greater blade area. These blade areas can be provided by increasing the propeller diameter, the number of blades, or the blade width.

Previous reports (references 1, 2, and 3) have presented the results of tests of propellers having from 2 to 8 normal-width blades. In references 1 and 2, the results were reported for propellers in the tractor position. In reference 3 the results were reported for propellers in the

pusher position. The present report presents results of tests of similar single- and dual-rotating tractor propellers of 50 percent greater blade width than those previously tested.

APPARATUS AND METHODS

The tests were made in the NACA 20-foot propeller-research wind tunnel with equipment that has been previously described in reference 1. A photograph of the test set-up is shown in figure 1. Figure 2 is a dimensioned plan drawing of the model.

Propellers.— The propeller blades used for the present investigation were identical in section, pitch distribution, and thickness ratio to the blades used in references 1, 2, and 3 but were 50 percent wider, except for the transition portion near the shank. The blades were made of wood and fitted into steel sleeves machined in accordance with SAE blade end no. 2 standard. They were finished with a white model enamel and rubbed to an aerodynamically smooth finish.

For identification purposes the blades will be referred to as "wide blades" and will be herein designated 3155-6-1.5 (right-hand) and 3156-6-1.5 (left-hand). The plan form and blade-form curves are given in figure 3 for the wide blades as well as for the standard-width 3155-6 blades.

The two-, three-, and four-blade single-rotating propellers were mounted on the rear hub only; whereas the six- and eight-blade single- and dual-rotating propellers and the four-blade dual-rotating propellers were mounted on separate hubs spaced 15 inches apart. Angular displacement between the front and the rear propeller blades for the single-rotation condition was the same for these tests as for previous tests on the standard blades. The front blade led the rear blade by 85.4° for the four-blade propeller, 75.0° for the six-blade propeller, and 52.5° for the eight-blade propeller. Reasons for the choice of these angles have been given in reference 3.

Test conditions.— The maximum tunnel speed (approximately 110 mph) and the power of the drive motors (two 25-hp electric motors) resulted in a Reynolds number and

L 585

a tip speed considerably below those experienced in flight. The maximum propeller speed, which was 550 rpm, was obtainable only for the low blade angles and the low range of advance-diameter ratios of the tests. The tip speed, consequently, was below 300 feet per second and the effect of compressibility could not therefore be measured. The Reynolds number of the 0.75 radius section was of the order of only one and one-half millions.

The same angular differences between the right-hand and left-hand propeller-blade settings were used for the dual-rotation tests with the wide blade as had been used with the standard-width blade. The left-hand (front) propeller was set at even values of blade setting and the right-hand (rear) propeller was set to absorb approximately the same power as the left-hand propeller for the peak-efficiency condition only. A plot of the angular difference between the front and the rear propeller-blade settings is given in figure 4. The rear propeller was set at the same blade angle as the front propeller for the 10° and the 15° blade angle. The speed of the right-hand propeller was maintained equal to the speed of the left-hand propeller throughout the tests. The test procedure was the same as the procedure used for investigations of references 1, 2, and 3.

RESULTS AND DISCUSSION

The measured values have been reduced to the usual coefficients of thrust, power, and propulsive efficiency,

$$C_T = \frac{\text{effective thrust}}{\rho n^2 D^4}$$

$$C_P = \frac{\text{engine power}}{\rho n^3 D^5}$$

$$\eta = \frac{C_T}{C_P} \times \frac{V}{nD}$$

$$C_S = \sqrt[5]{\frac{\rho V^5}{P n^2}} \quad \text{or} \quad \sqrt[5]{\frac{V/nD}{C_P}}$$

where

P power absorbed by propeller, foot-pounds per second
 V airspeed, feet per second
 n propeller rotational speed, revolutions per second
 D propeller diameter, feet
 ρ mass density of the air, slugs per cubic foot

The effective thrust is the measured thrust of the propeller-body combination plus the drag of the body measured separately.

Several comparisons have been made on a basis of the activity factor for the propeller unit, expressed as

$$\text{Total activity factor} = B \times \frac{100000}{16} \int_{0.2}^{1.0} \left(\frac{r}{R}\right)^3 \frac{b}{D} d\left(\frac{r}{R}\right)$$

where

b blade width, feet

r radius to any station along blade, feet

R radius of propeller, feet

B number of blades

The figures giving the basic propeller characteristics are presented in the following table:

Figure	Number blades	Rotation	Remarks
5 to 8	2	single	Tested in rear hu
9 to 12	3	single	Do.
13 to 16	4	single	Do.
17 to 21	4	dual	
22 to 25	6	single	
26 to 30	6	dual	
31 to 34	8	single	
35 to 39	8	dual	

Various comparisons and design charts are presented in figures 40 to 62, as follows:

Figure

- 40 Effect of dual rotation on efficiency envelopes
- 41 Variations in efficiency gain due to dual rotation with solidity and V/ND
- 42 to 44 Effect of dual rotation on efficiency at constant power
- 45 Efficiency-envelope comparisons for different solidities
- 46 to 52 Effect of solidity on efficiency at constant power
- 53 Efficiency-envelope comparisons for propellers having the same solidity but a different number of blades
- 54 to 55 Effect of number of blades on efficiency at constant power and solidity
- 56 to 60 Variation of thrust-coefficient with activity factor
- 61 Design chart for propellers 3155-6-1.5 and 3156-6-1.5 of different solidities; single rotation
- 62 Design chart for propellers 3155-6-1.5 and 3156-6-1.5 of different solidities; dual rotation

Effect of dual rotation.—The effects of dual rotation appear to be about the same for wide blades as noted for the standard blades reported in references 1, 2, and 3. These effects may be studied closely by referring to the basic propeller characteristics given in figures 17 to 39 wherein results from the single-rotation tests are superimposed on the results from the dual-rotation tests for three representative angles.

A comparison of the envelope curves for single- and dual-rotating propellers of the same solidity is given in figure 40. The four-blade dual-rotating propeller was from 1 to 3 percent more efficient than the single-rotating propeller; whereas the six-blade propeller was from 3 to 4 percent more efficient. The gain in efficiency through dual rotation was slightly less for the eight-blade propeller than for the six-blade propeller. As this result seemed contrary to established trends (see figure 41) and also to theoretical considerations, it was thought that some of the results might be in error. Repeat tests, however, of both the six- and the eight-blade propellers checked the original tests.

The gains through dual rotation, for equal solidities, were roughly the same for the wide blades (fig. 41) as for the standard blades previously tested. Small differences noted are within the experimental accuracy.

The results of references 1 and 2 have indicated that the gains due to dual rotation would be expected to be about twice as great for the condition with the wing removed as for the condition with the wing in place. The gains would also be expected to be greater for the pusher position than for the tractor position. (See reference 3.)

Since dual-rotating propellers absorb slightly more power than single-rotating propellers, a slightly better comparison of the effect of dual rotation on efficiency is provided in figures 42 to 44 wherein comparisons are made on the basis of constant C_p . The gain through dual rotation was more pronounced for the take-off and climbing conditions than for high speed, especially at high values of C_p .

Effect of solidity.— The efficiency envelope curves in figure 45, which represent a blade efficiency, lead to the same general conclusions as similar curves in references 1 to 3. An increase in solidity due to an increase in the number of blades from two to eight resulted in a loss of blade efficiency amounting to as much as 6 percent for single rotation. The difference in efficiency due to the change from a six- to an eight-blade propeller was apparently less than the percentage accuracy of testing, since the same envelopes were faired through both sets of curves. With dual rotation, the loss in blade efficiency due to increased solidity was less in general than for single rotation; the loss was, however, appreciable.

It was realized that efficiency envelopes based solely on V/nD served as an unfair basis of comparison for the propeller as a whole because, for any given value of advance-diameter ratio, the power absorbed was nearly proportional to the number of blades. In figures 46 to 52, therefore, the efficiency comparisons for the various propellers have been plotted at certain assumed values of the power coefficient. For the take-off and climb conditions, there was an appreciable increase in efficiency with increasing number of blades, particularly for the higher power coefficients. For a propeller designed to give the best performance at high speed, some loss in efficiency at high speed is unavoidable if the solidity is increased to improve the take-off.

As a first approximation, the effect of increasing the solidity may be considered to be the same whether this increase is obtained by varying either the blade width or the number of blades. Modern theory (references 4 and 5) indicates, however, that for a given solidity the efficiency will increase with the number of blades. The present experiments indicate, nevertheless, that the differences in efficiency were small and were, in general, within the experimental error. (See figs. 53 to 55.)

The problem often arises in design work of correcting propeller-performance computations for differences in activity factor between the propeller that is being used and the propeller for which test results are available. In order to facilitate such corrections, plots of C_T against activity factor for constant values of C_p are included for several values of V/nD . (See figs. 56 to 60.) The plot for $V/nD = 0$ is not included because the results from static thrust tests are not yet available.

The results for both standard and wide blades, which are included, allow a fairly accurate estimate of the effect of changes in activity factor on thrust. The results for wide blades agree fairly well with the results for the standard blades except in the stalling range, where the wide blades exhibit a higher thrust for a given power coefficient.

Composite C_S charts.— In figure 61 is presented a composite of the envelopes of C_S charts for single-rotating propellers and in figure 62, a composite for dual-rotating propellers. The figures may serve as an aid in

preliminary design for the selection of a suitable propeller and should be used in conjunction with a speed-advance-diameter ratio chart, such as figure 58 of reference 3, from which a value of V/ND may be found for the limiting tip speed. Efficiencies and diameters may be determined for several solidities from the composites. These charts provide a measure of the relative diameter of different propellers having a different number of blades as well as a comparison of the efficiency of propellers selected on a basis of C_s , irrespective of the diameter.

CONCLUSIONS

1. The maximum efficiency for extremely high solidity propellers was relatively high. A propeller having a total activity factor of 1076 had a maximum efficiency of 83 percent for single rotation and 85 percent for dual rotation, as compared with 88 percent for a conventional three-blade propeller having an activity factor of 269.
2. The general effects of dual rotation found in this investigation of wide-blade propellers differed little from the effects found in previous reports on standard-blade propellers. These effects are summarized as follows:
 - (a) Dual-rotating propellers absorbed substantially more power for the peak-efficiency condition than single-rotating propellers of the same solidity; the effect was even more pronounced for the take-off and climb conditions.
 - (b) Dual-rotating propellers were found to be substantially more efficient for the take-off and climbing conditions of flight than the single-rotating propellers, particularly for operation at high power coefficients.
3. The general effects of changes in number of blades found in this investigation of wide-blade propellers agree with results of investigations on standard-blade propellers. These effects are summarized as follows:
 - (a) The peak blade efficiency was found to decrease with increased number of blades; this effect

was more pronounced for single-rotating propellers than for dual-rotating propellers.

- (b) The efficiency for the take-off and climbing conditions increased substantially with increased number of blades for constant power input with a slight loss at the high-speed condition.

4. The peak efficiency for a four-blade single- or dual-rotating propeller was found to differ from a six-blade propeller of the same solidity by not more than 1 or 2 percent.

Langley Memorial Aeronautical Laboratory,
National Advisory Committee for Aeronautics,
Langley Field, Va.

REFERENCES

1. Biermann, David, and Hartman, Edwin P.: Wind-Tunnel Tests of Four- and Six-Blade Single- and Dual-Rotating Tractor Propellers. NACA Rep. No. 747, 1948.
2. Biermann, David, and Gray, W. H.: Wind-Tunnel Tests of Eight-Blade Single- and Dual-Rotating Propellers in the Tractor Position. NACA ARR, Nov. 1941.
3. Biermann, David, and Gray, W. H.: Wind-Tunnel Tests of Single- and Dual-Rotating Pusher Propellers Having from Two to Eight Blades. NACA ARR, Feb. 1942.
4. Hartman, Edwin P., and Biermann, David: The Aerodynamic Characteristics of Full-Scale Propellers Having 2, 3, and 4 Blades of Clark Y and R.A.F. 6 Airfoil Sections. NACA Rep. No. 640, 1938.
5. Glauert, H.: Airplane Propellers. Vol. IV, div. L of Aerodynamic Theory, W. F. Durand, ed., Julius Springer (Berlin), 1935, pp. 169-360.

NACA

FIG. 1

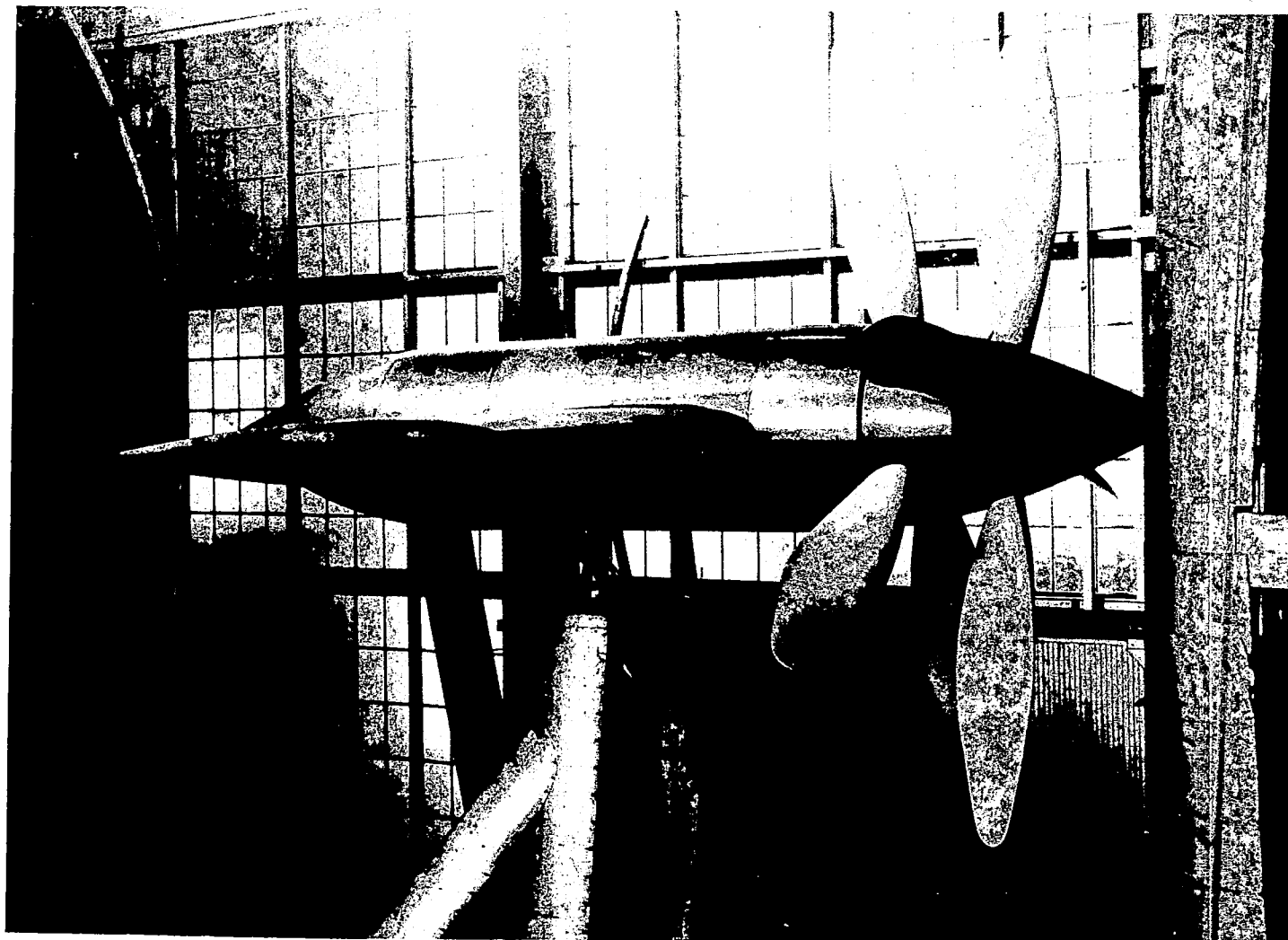


Figure 1.- Test set-up. Eight-blade dual-rotating propeller with wing.

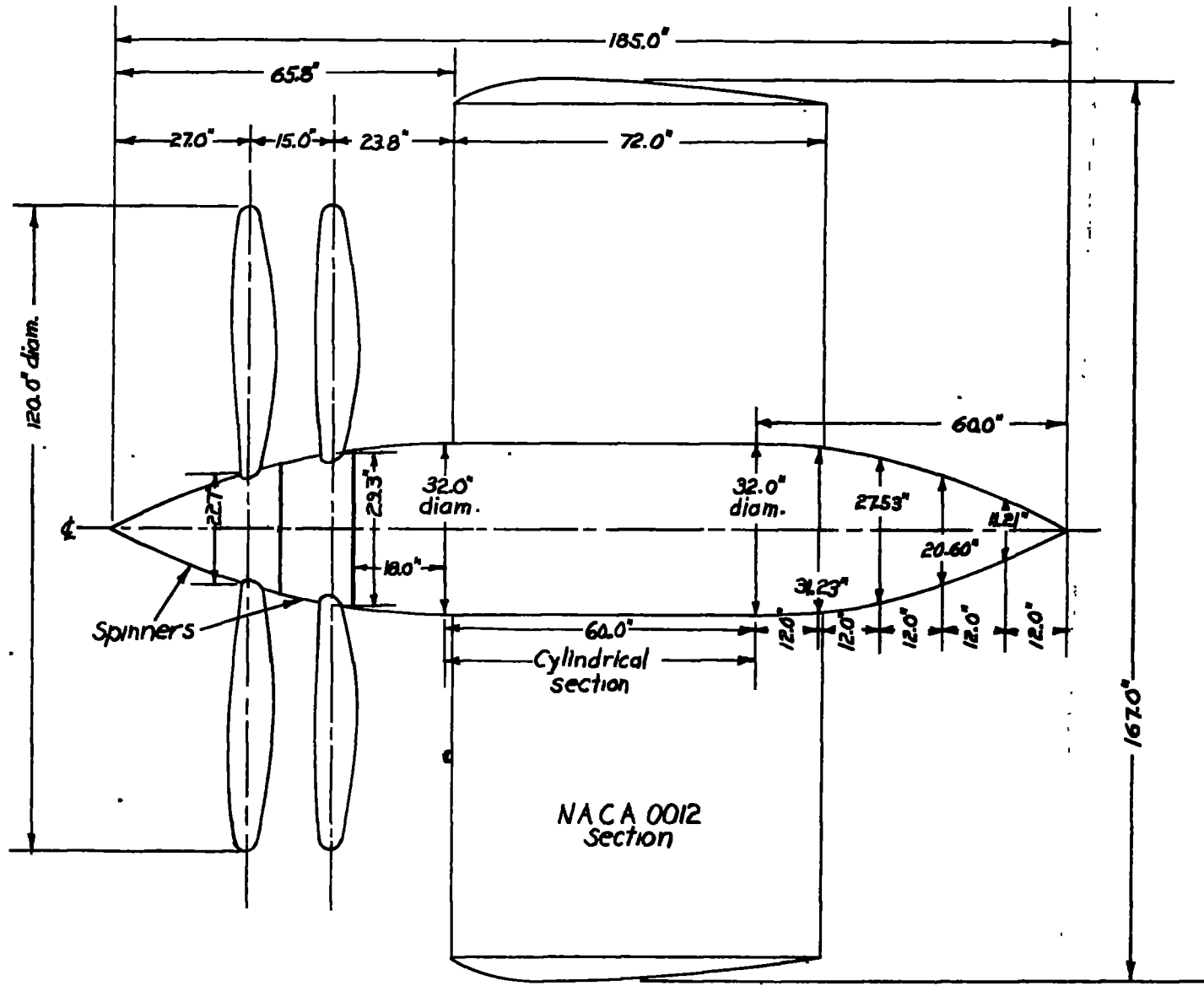


Figure 2.- Plan view showing dimensional details of wing and nacelle.

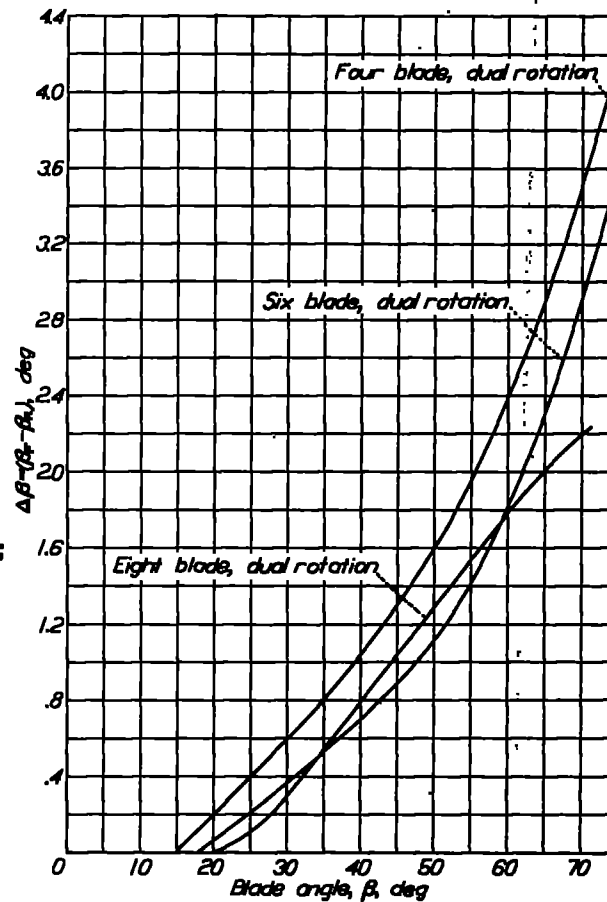
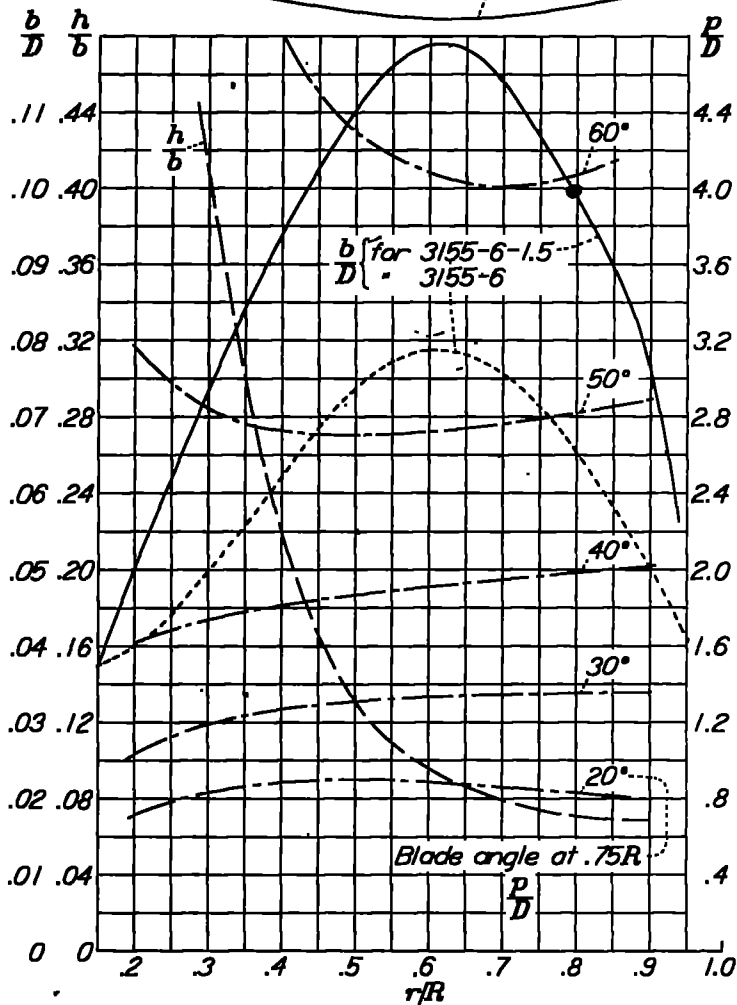
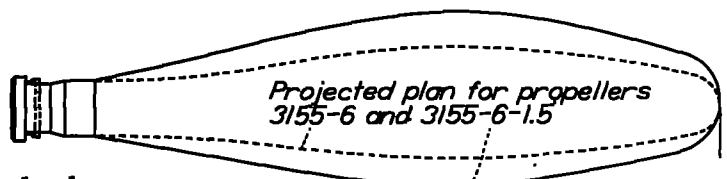


Figure 4.-Difference in blade angle at 0.75R for equal torque at peak efficiency.

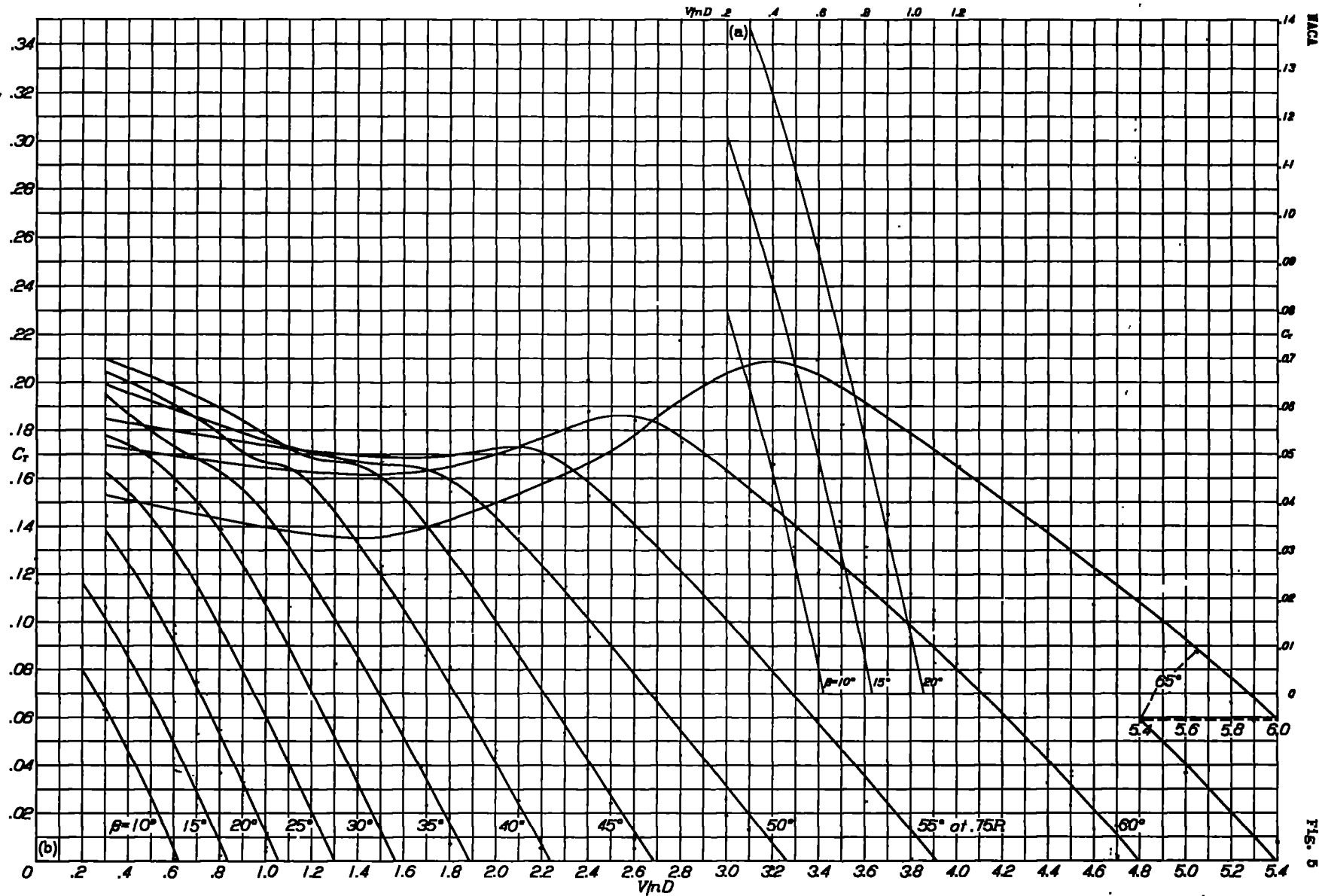


Figure 5.- Thrust-coefficient curves for two-blade single-rotating propeller.

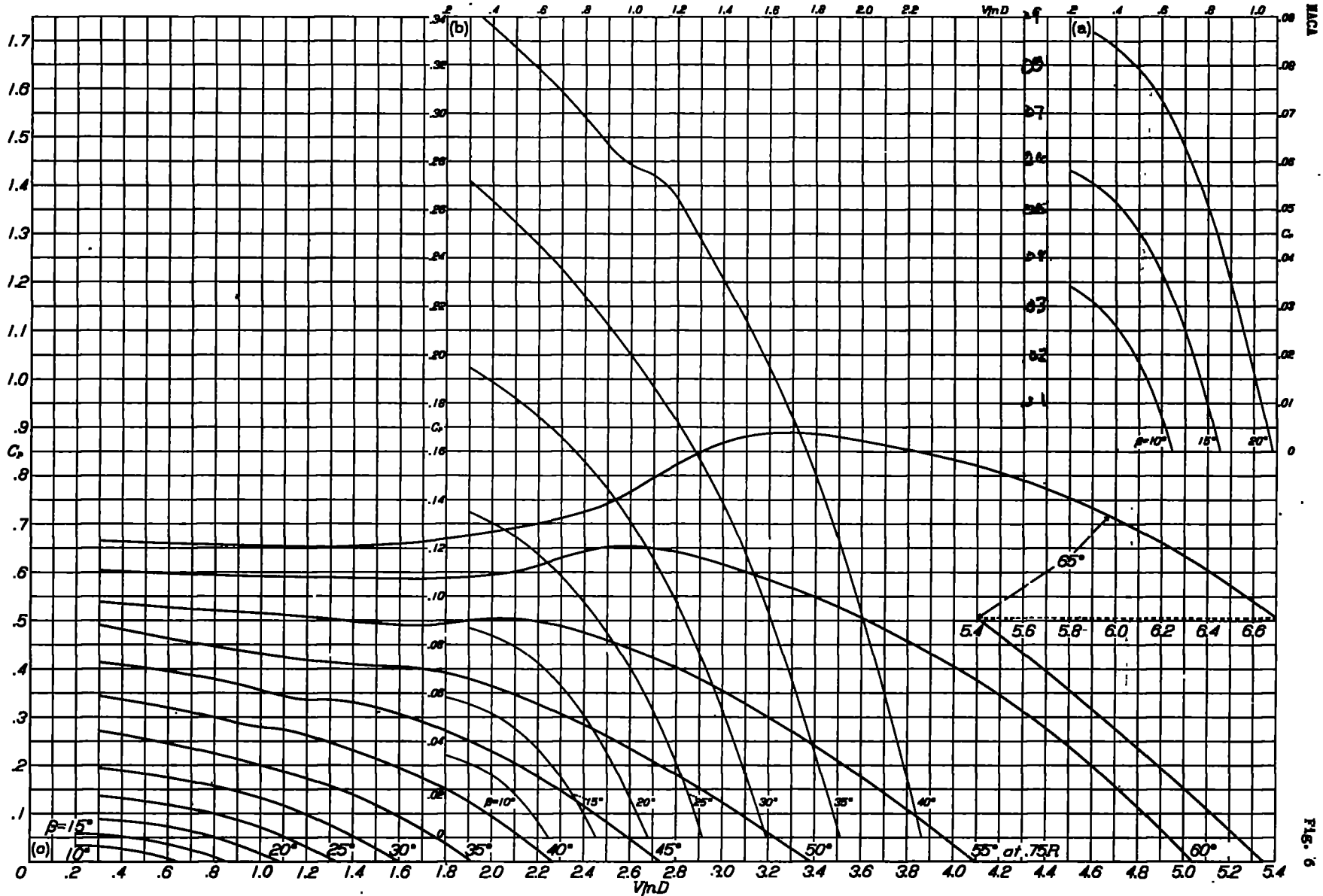


Figure 6.- Power-coefficient curves for two-blade single-rotating propeller.

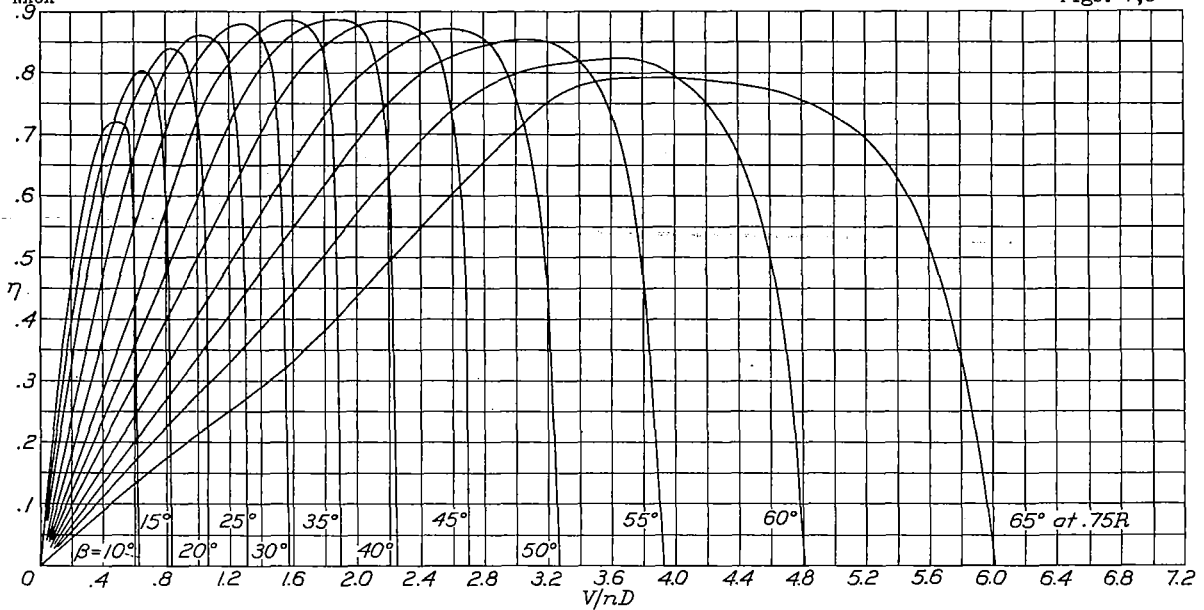


Figure 7.- Efficiency curves for two-blade single-rotating propeller.

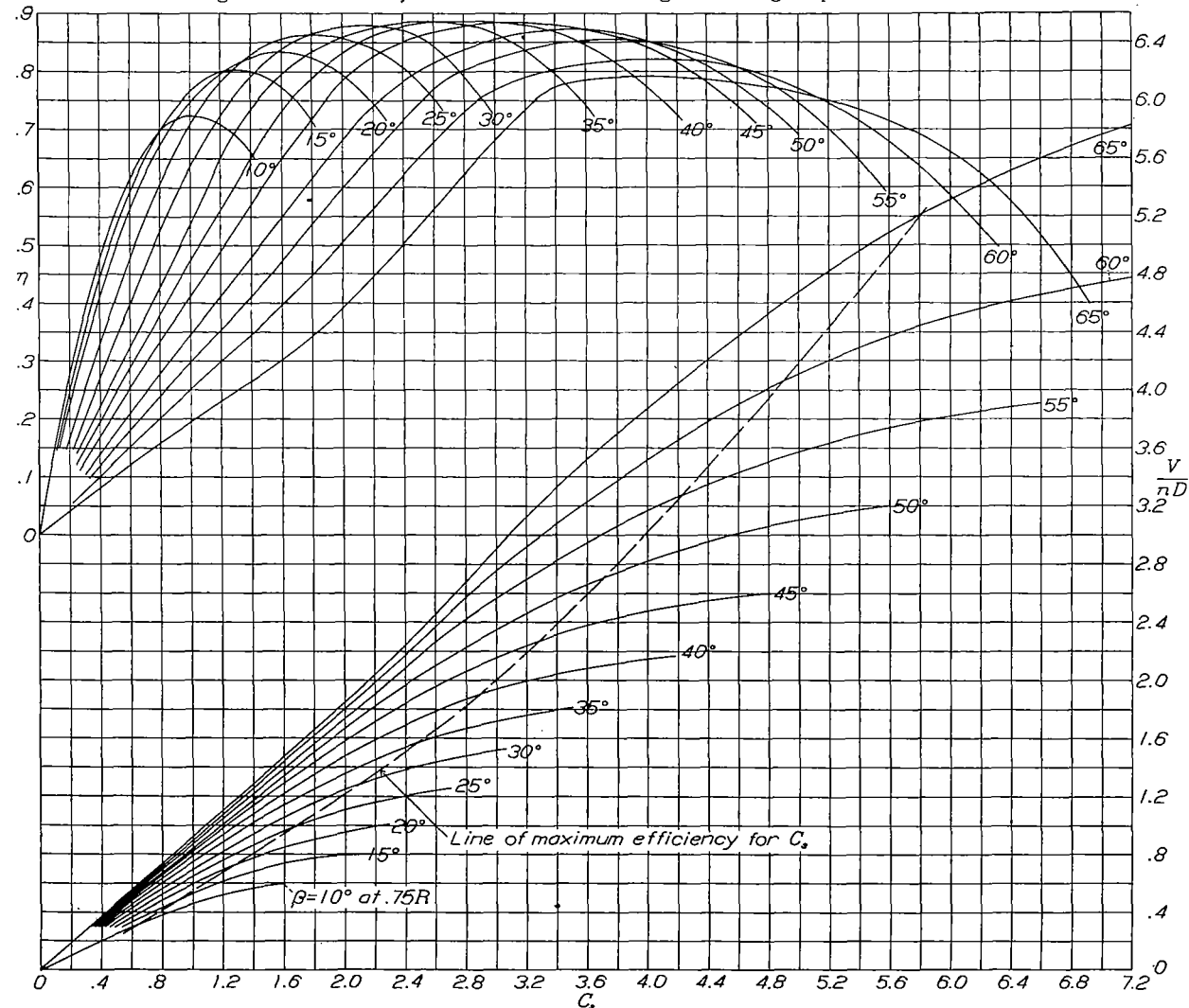


Figure 8.- Design chart for propeller 3155-6-1.5; two blades.

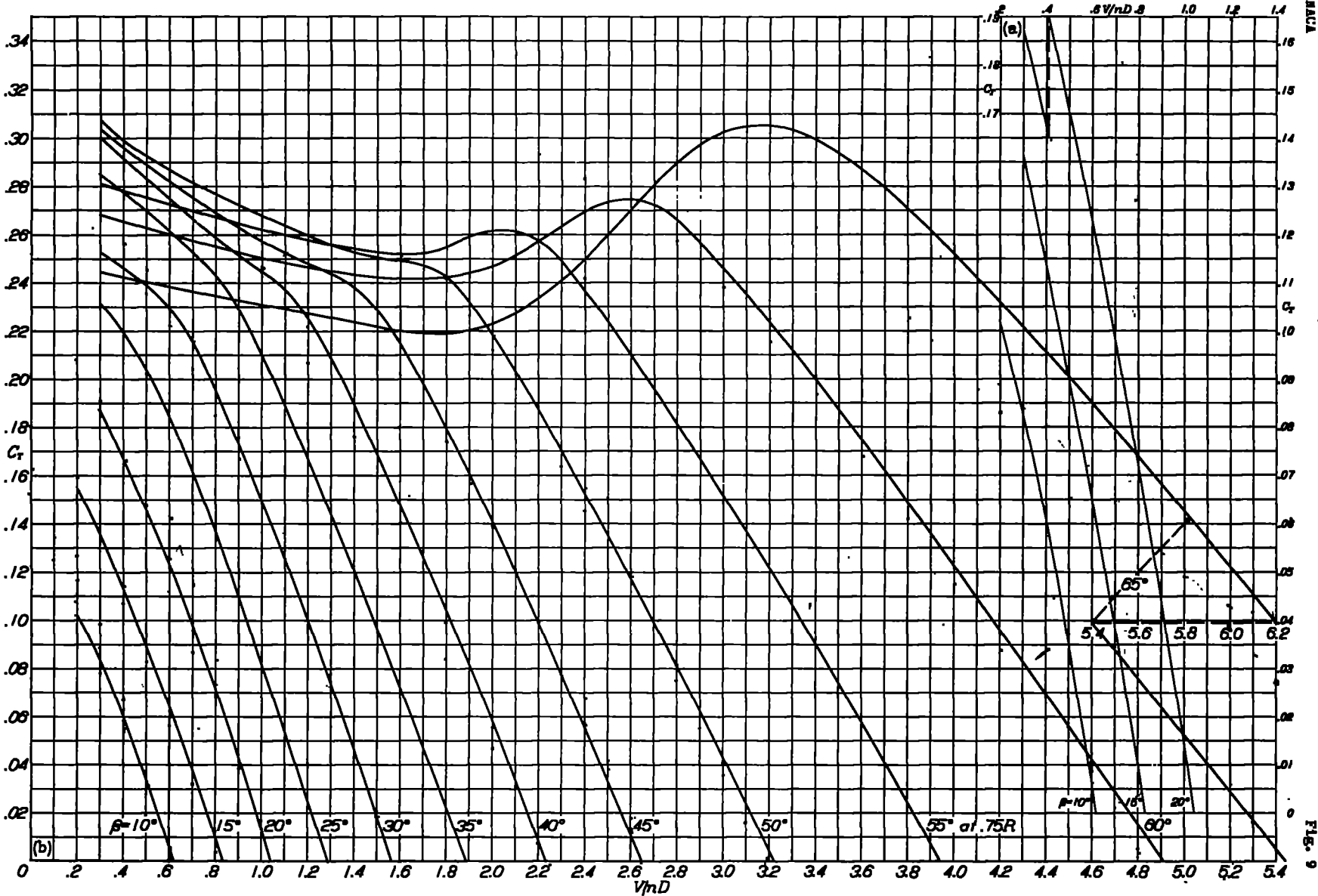


Figure 9.- Thrust-coefficient curves for three-blade single-rotating propeller.

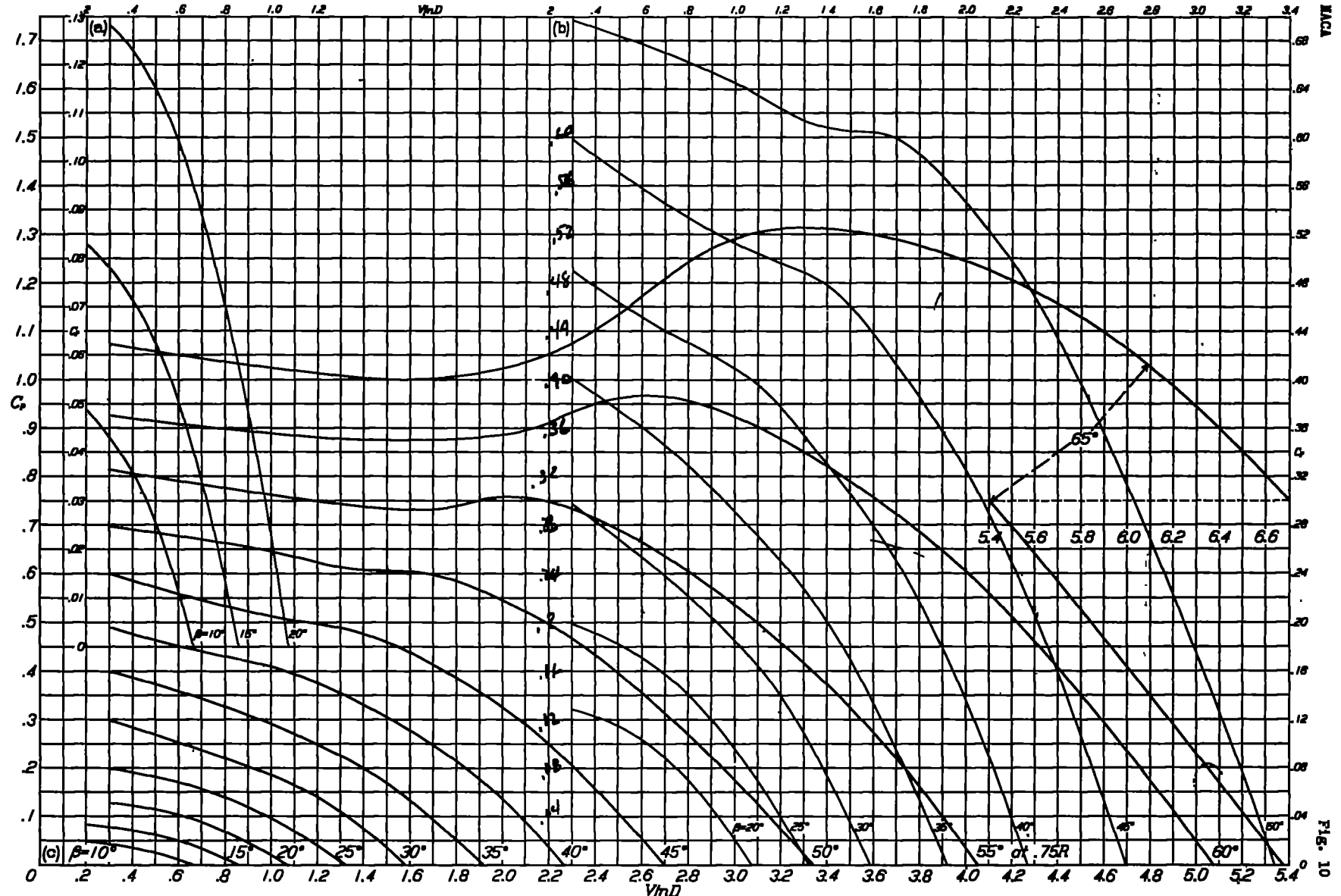


Figure 10. Power-coefficient curves for three-blade single-rotating propeller.

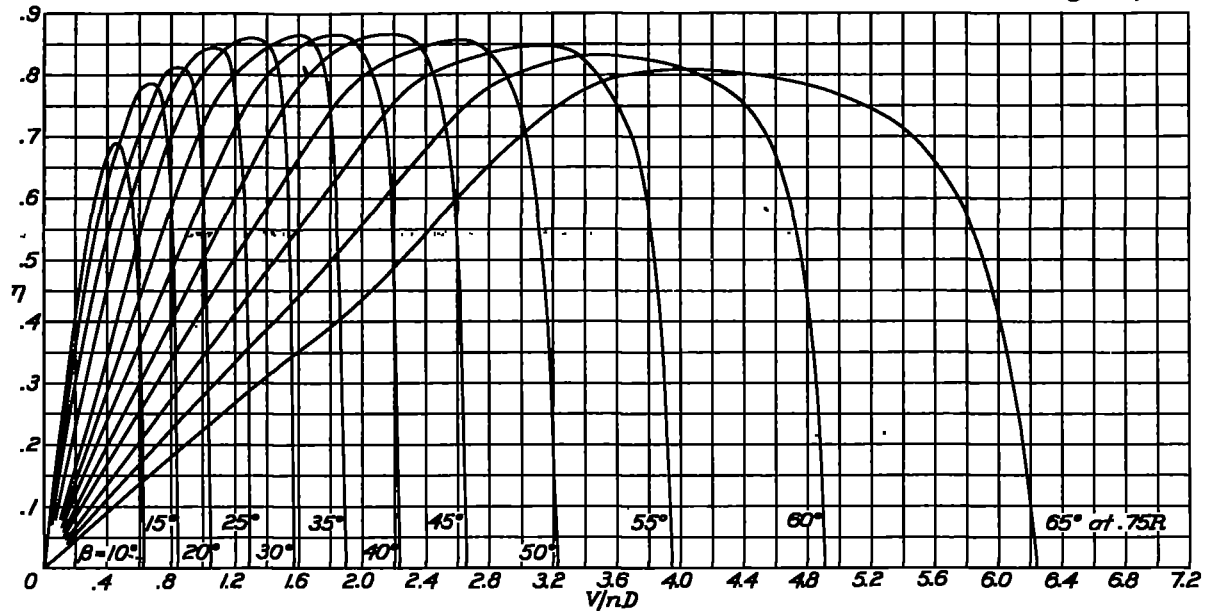


Figure 11.- Efficiency curves for three-blade single-rotating propeller.

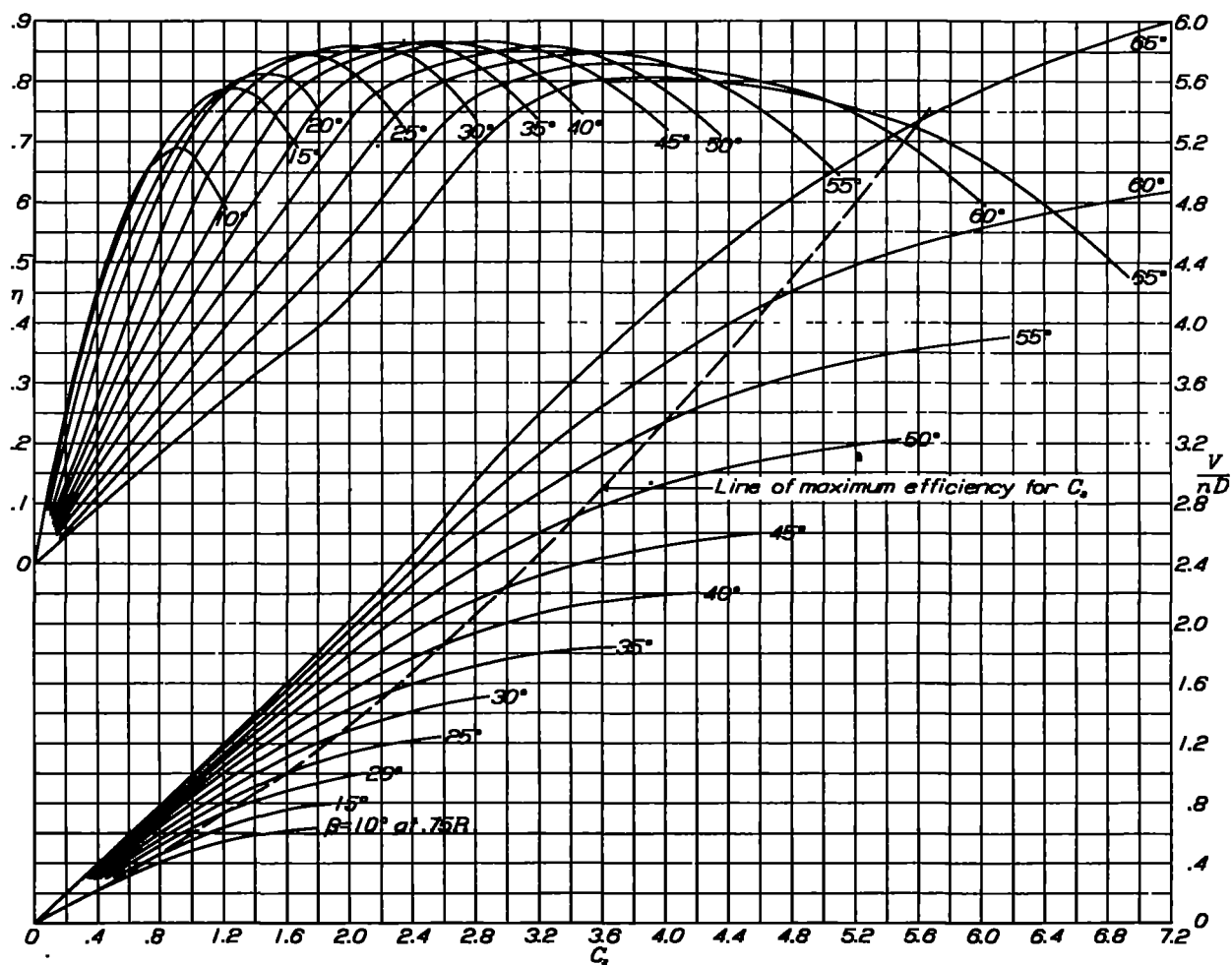


Figure 12.- Design chart for propeller 3155-6-1.5; three blades.

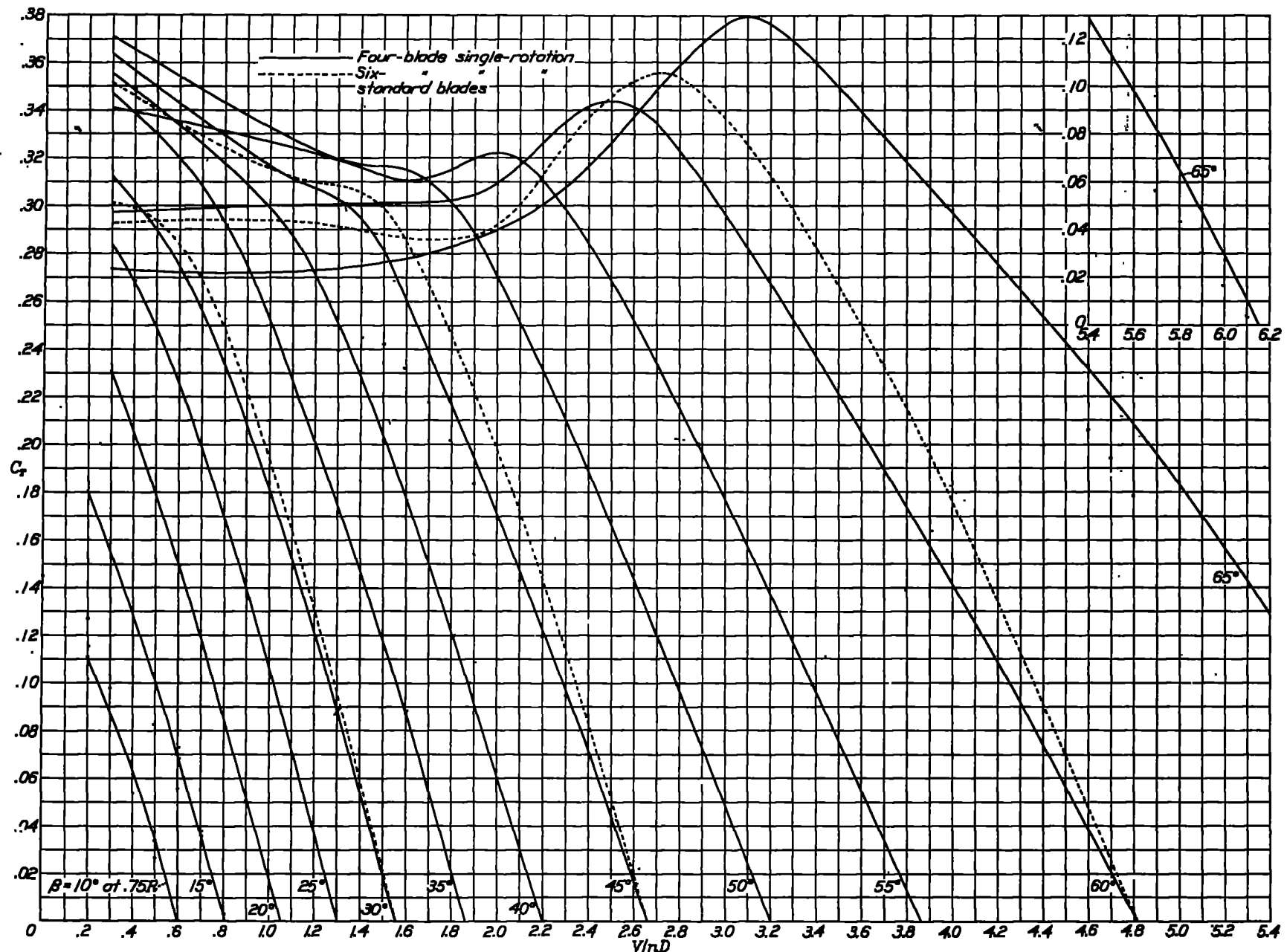


Figure 13.- Thrust-coefficient curves for four-blade single-rotating propeller.

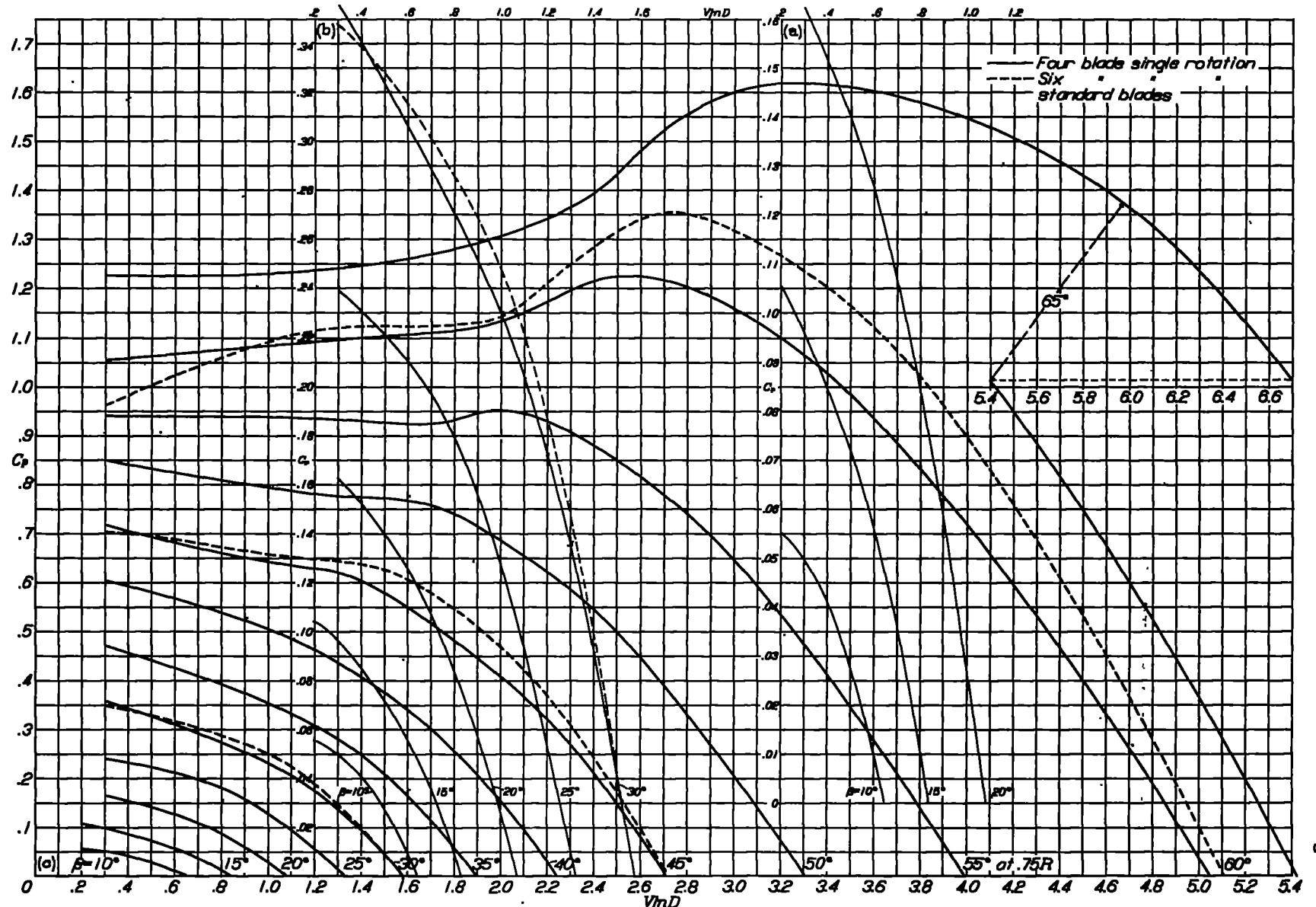


Figure 14.- Power-coefficient curves for four-blade single-rotating propeller.

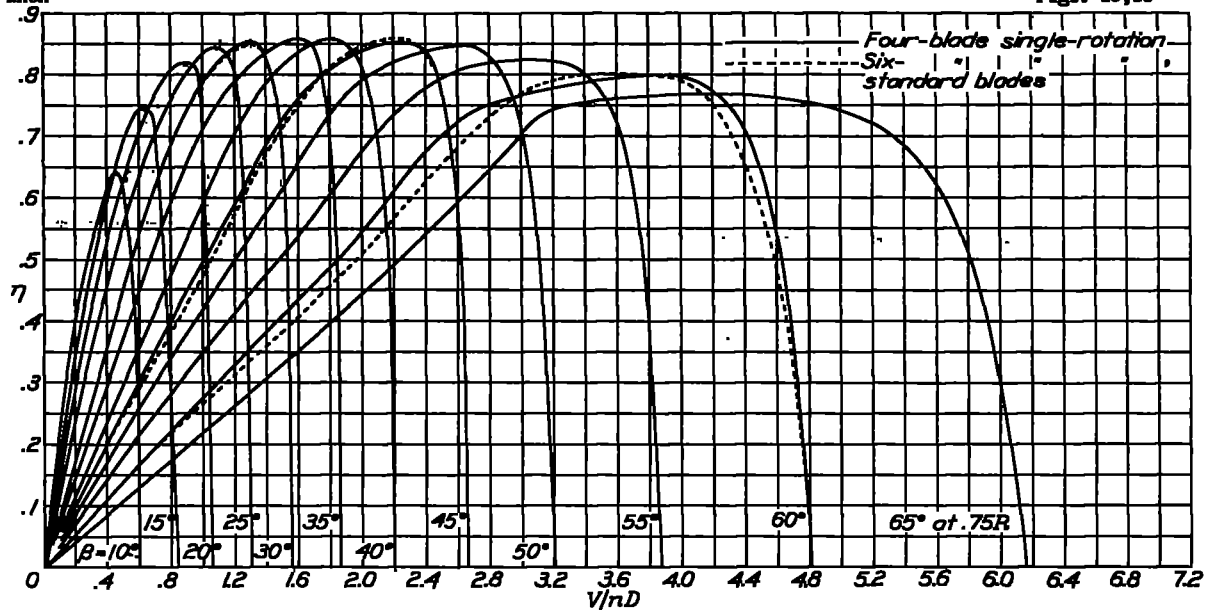


Figure 15.- Efficiency curves for four-blade single-rotating propeller.

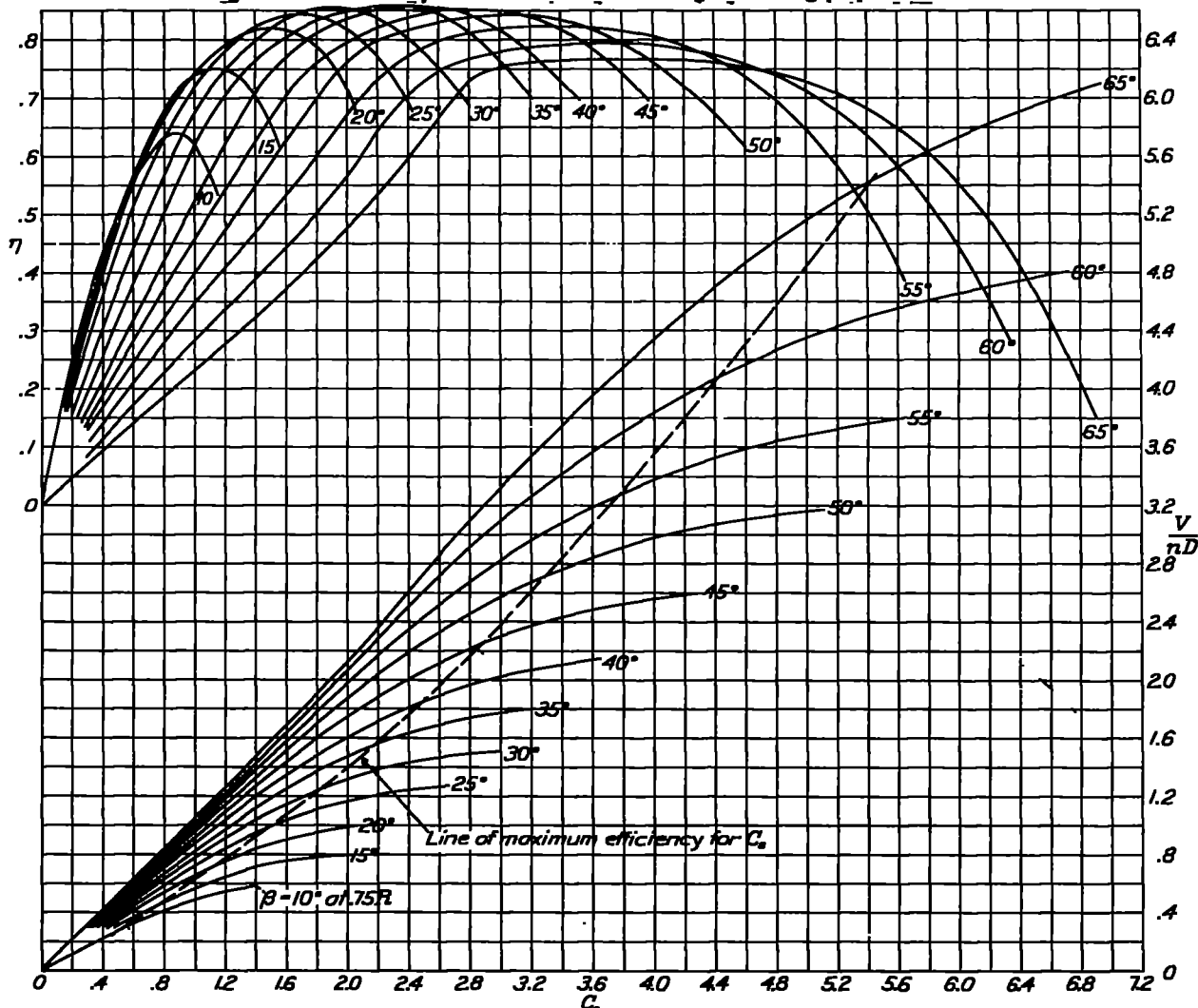


Figure 16.- Design chart for propeller 3153-6-1.5; four blade; single rotation.

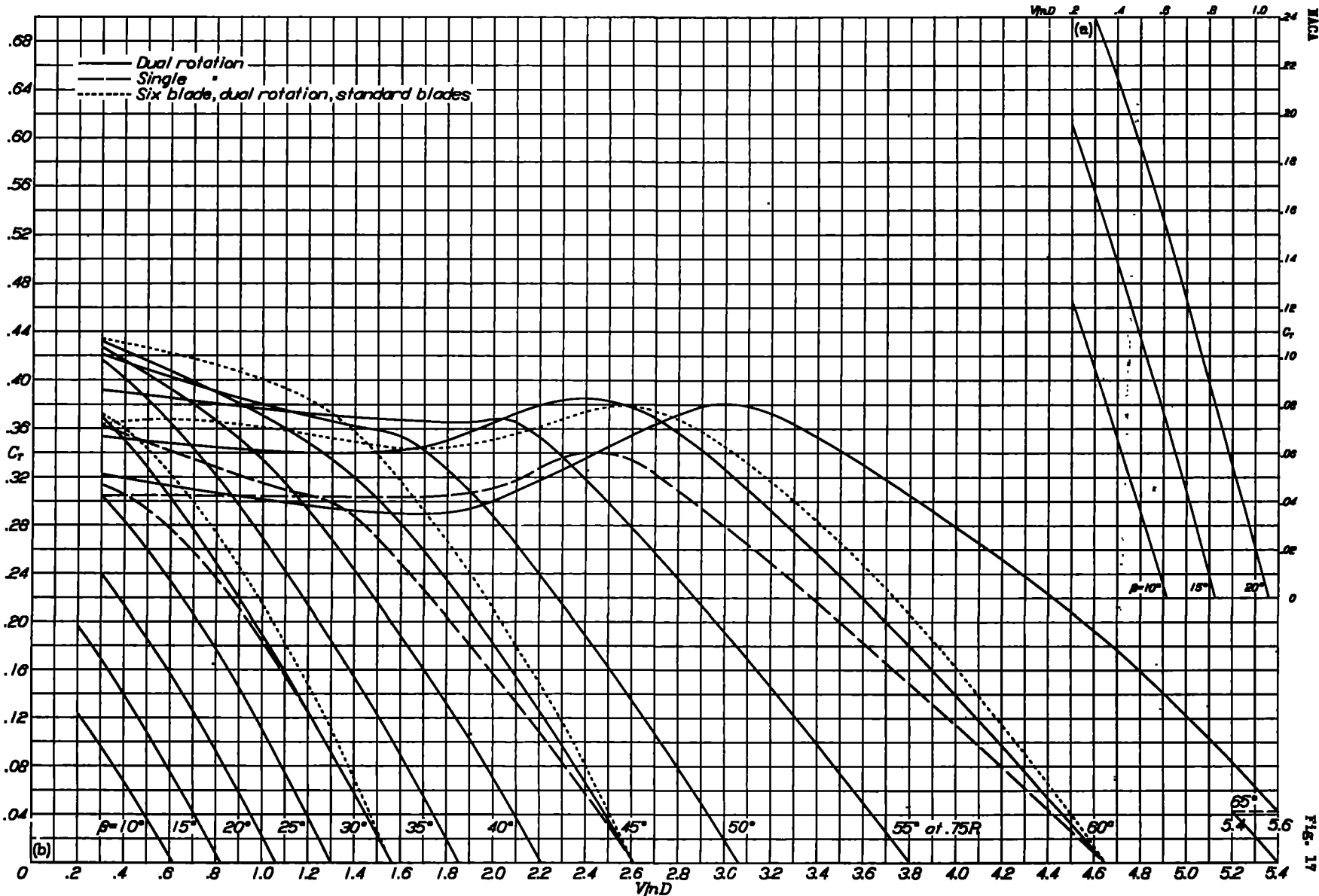


Figure 17.- Thrust -coefficient curves for four-blade dual-rotating propeller, showing superimposed curves for 30° , 45° , and 60° single rotation.

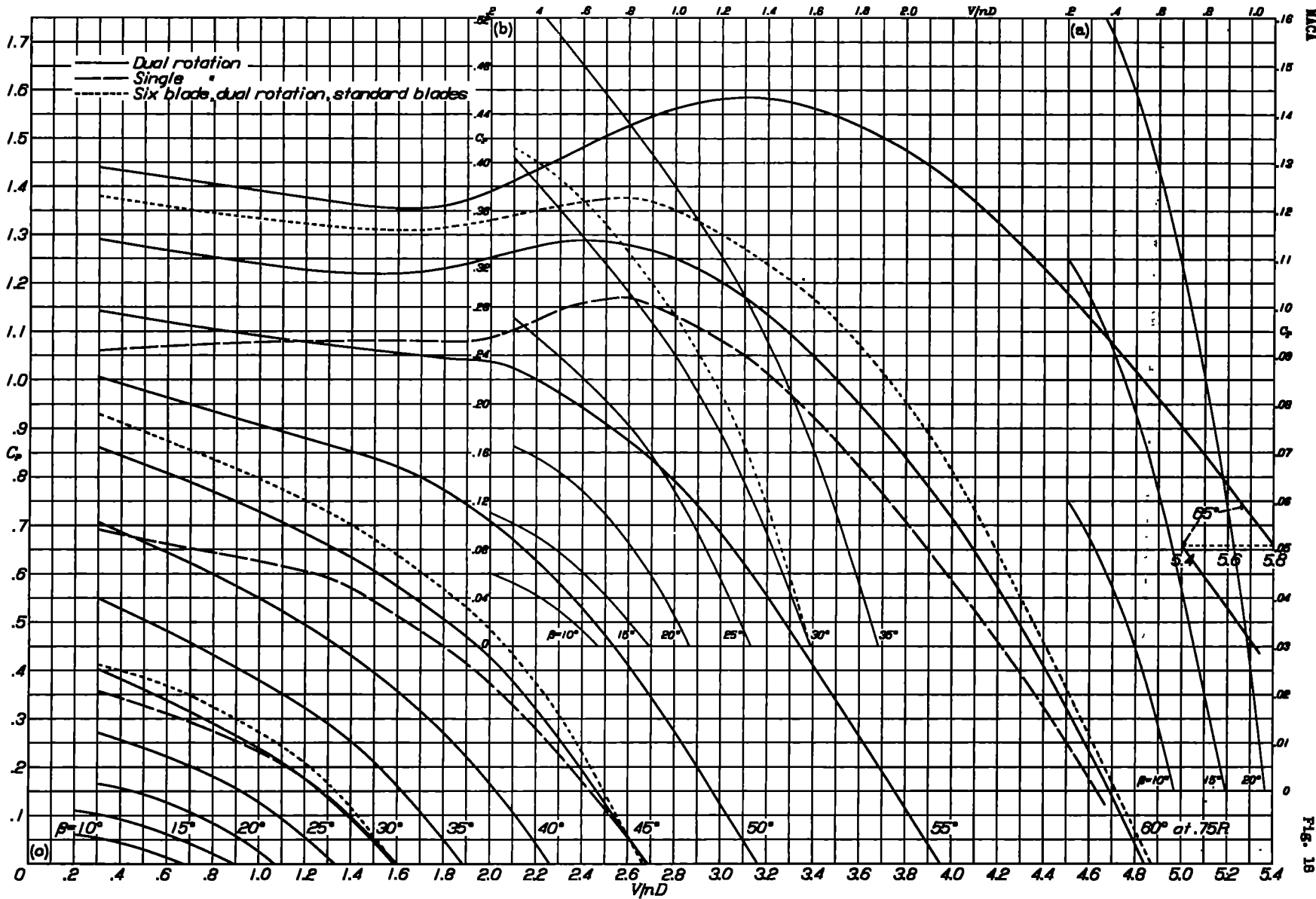


Figure 18.- Power-coefficient curves for four-blade dual-rotating propeller, showing superimposed curves for 30° , 45° , and 60° single rotation.

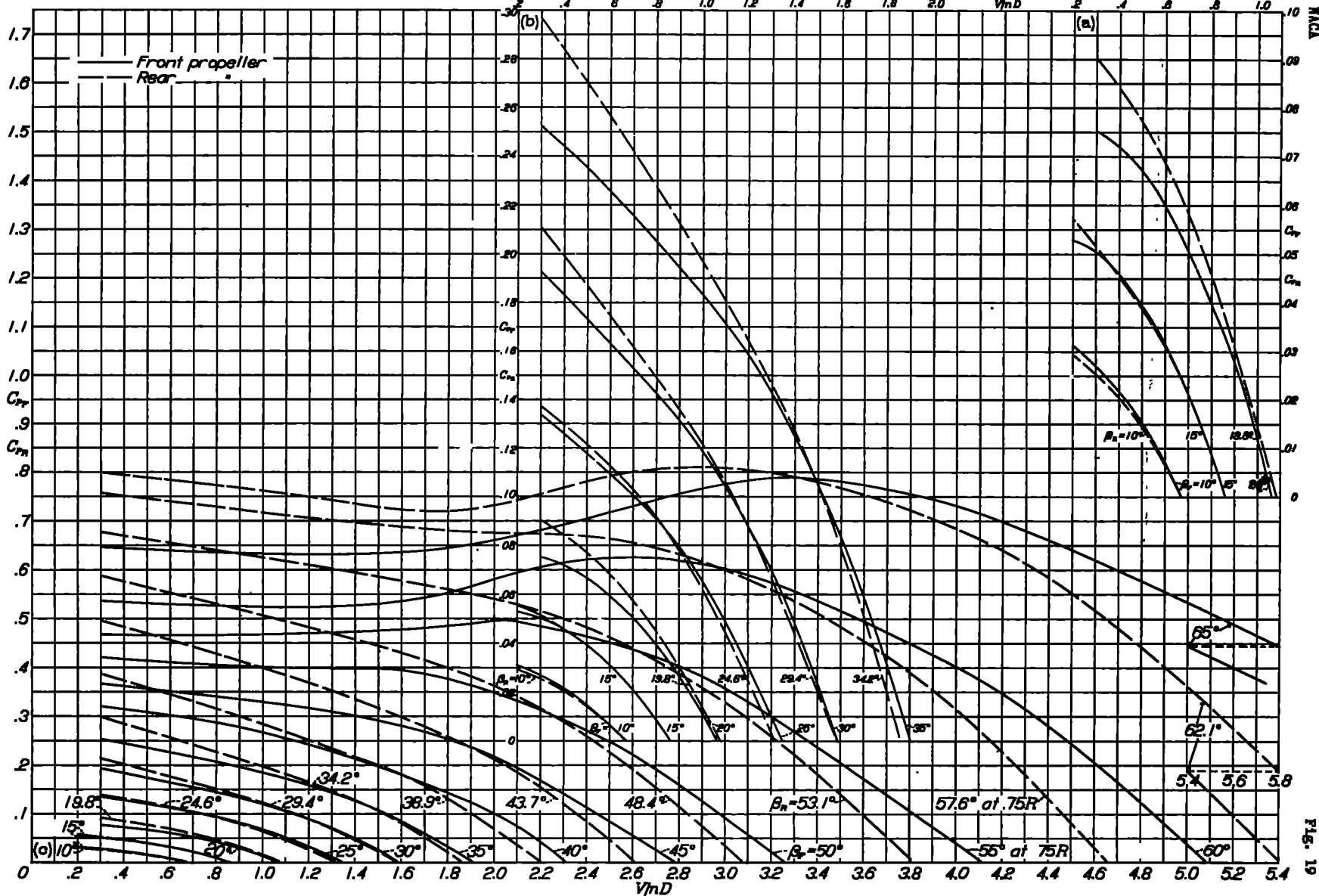


Fig. 20, 21

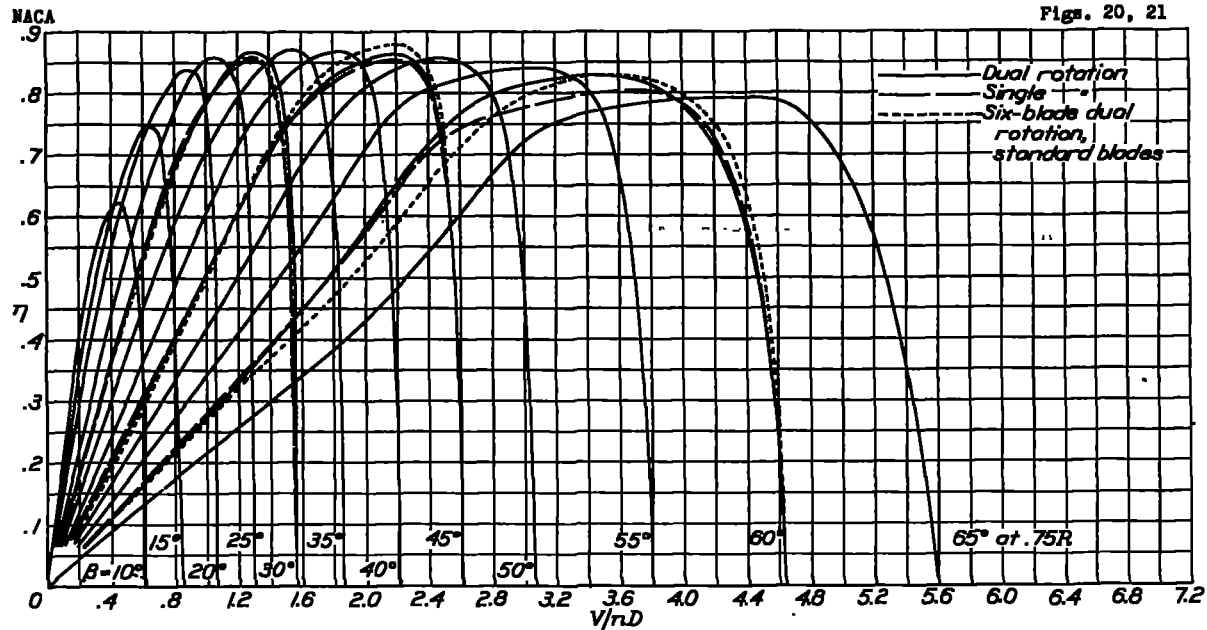


Figure 20.- Efficiency curves for four-blade dual-rotating propeller, showing curves for 30°, 45°, and 60° single rotation.

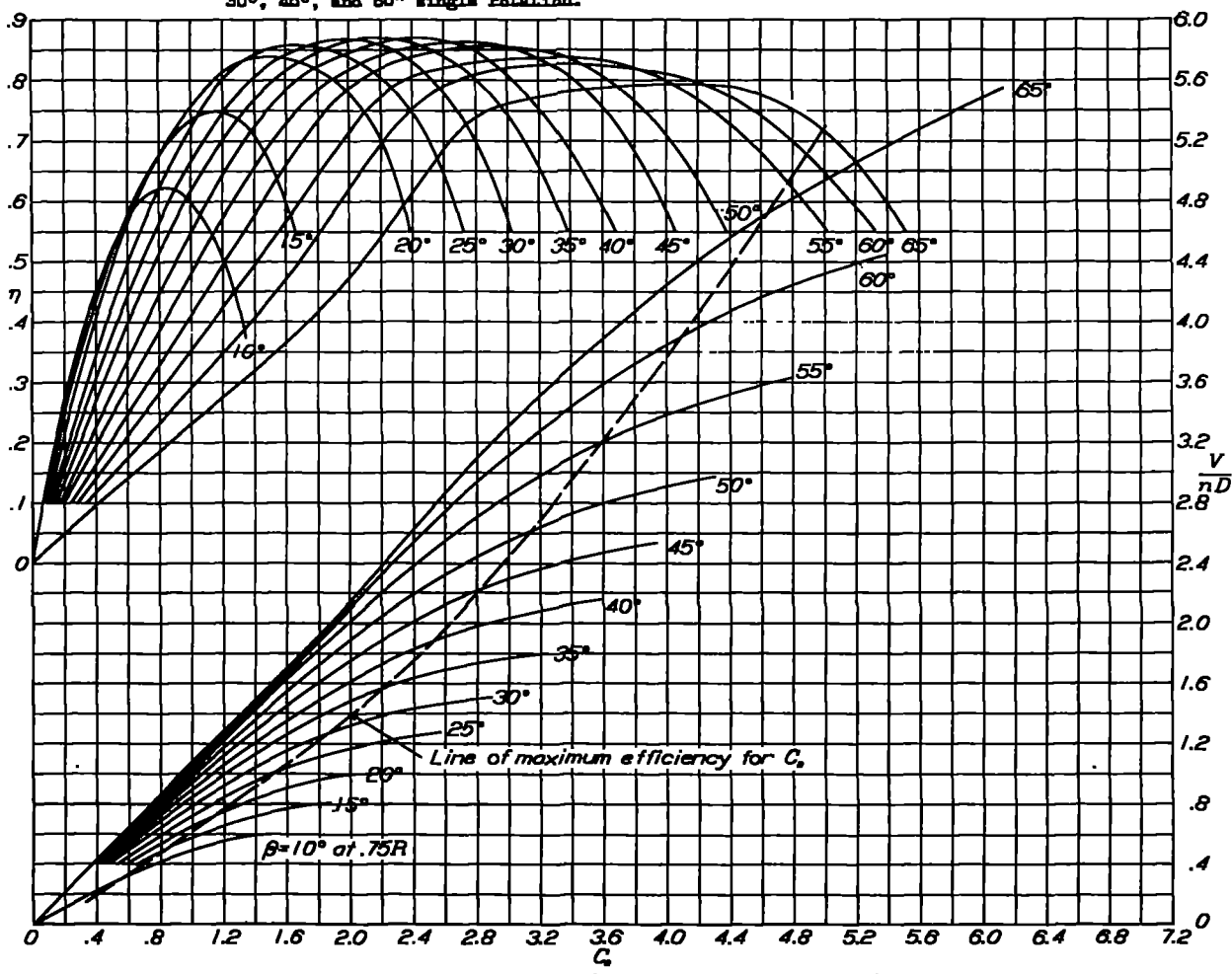


Figure 21.- Design chart for propellers 3156-6-1.5 (R.H.) and 3156-6-1.5 (L.H.), four blade dual rotation.

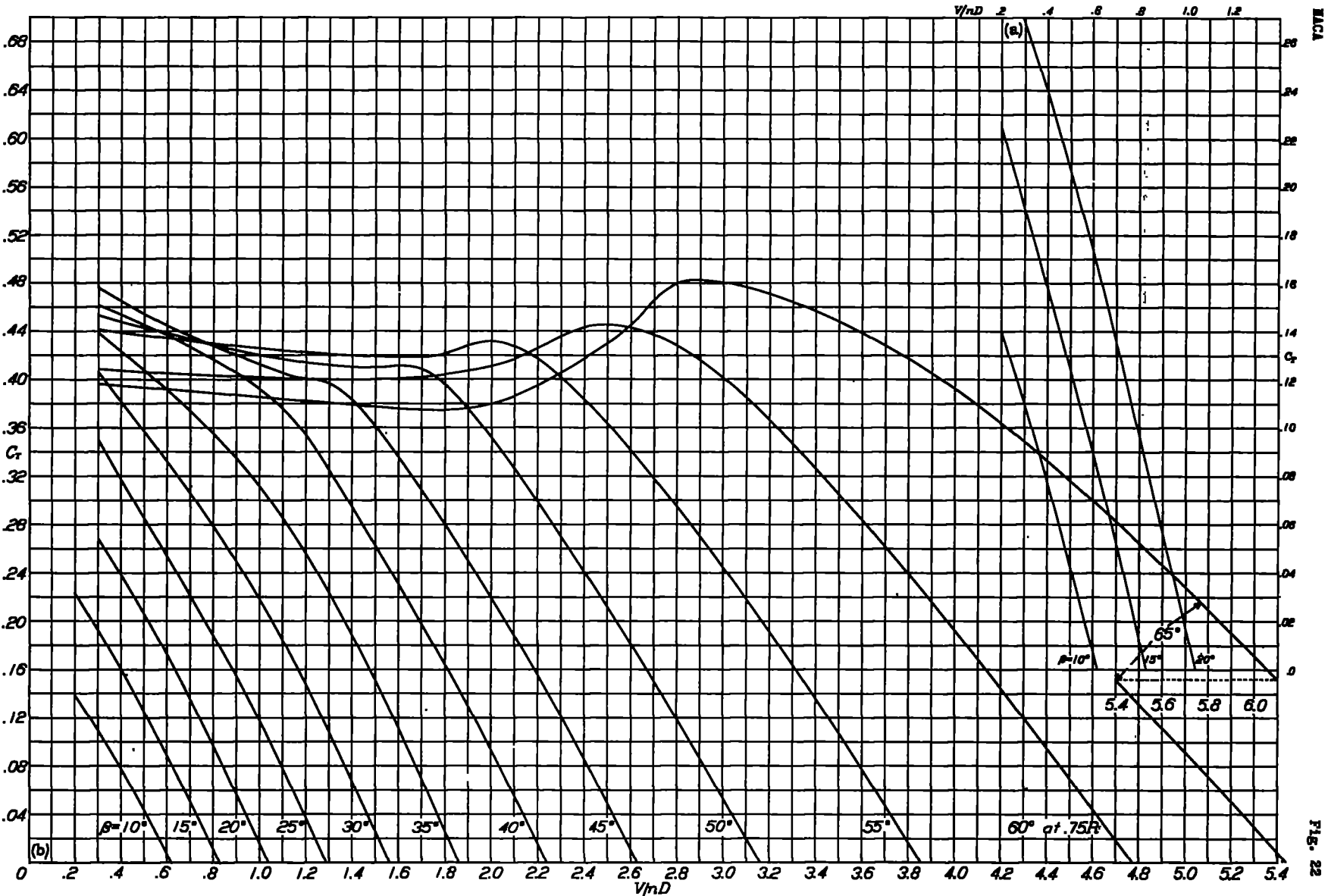


Figure 22.- Thrust-coefficient curves for six-blade single-rotating propeller.

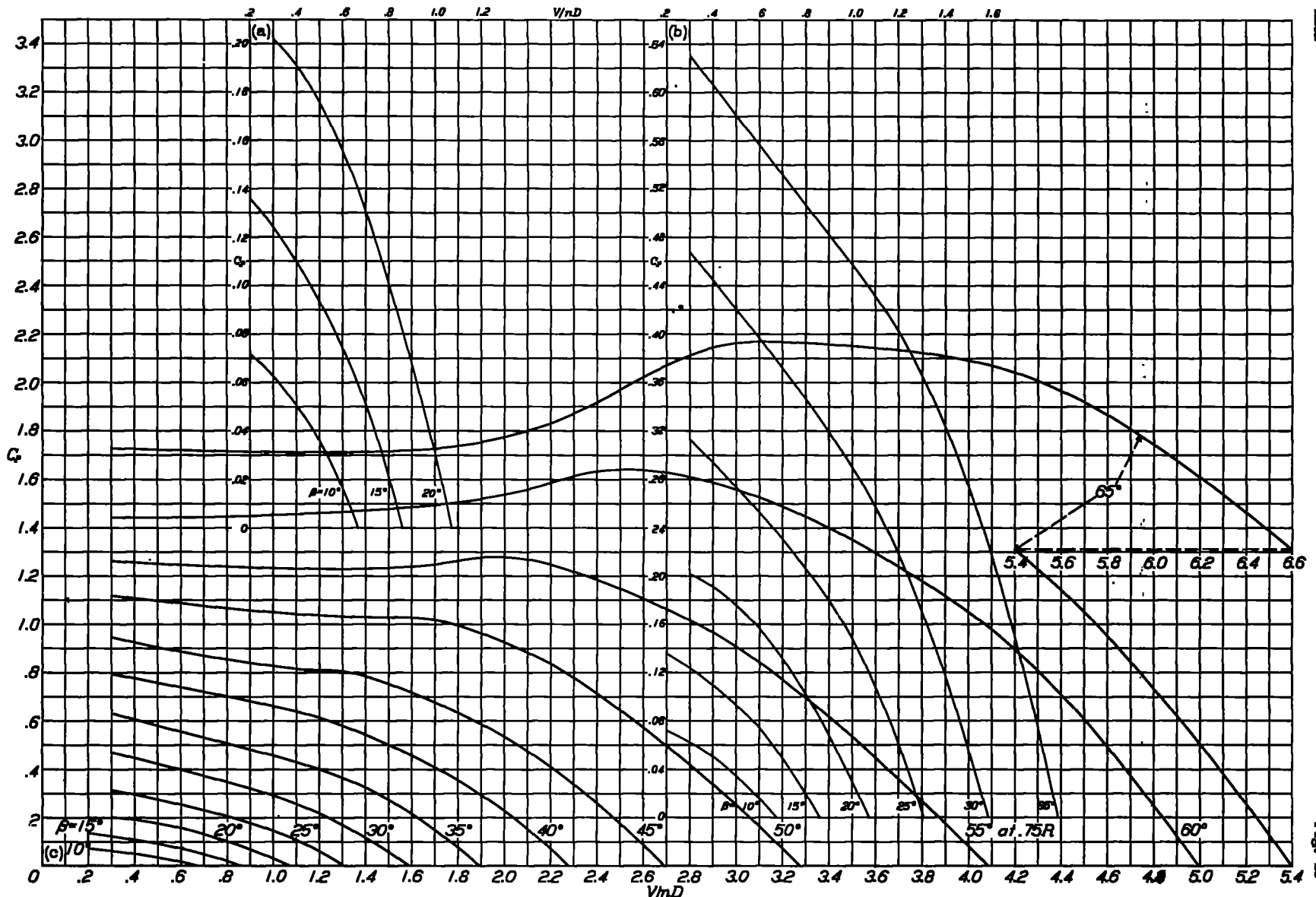


Figure 25.- Power-coefficient curves for six-blade single-rotating propeller.

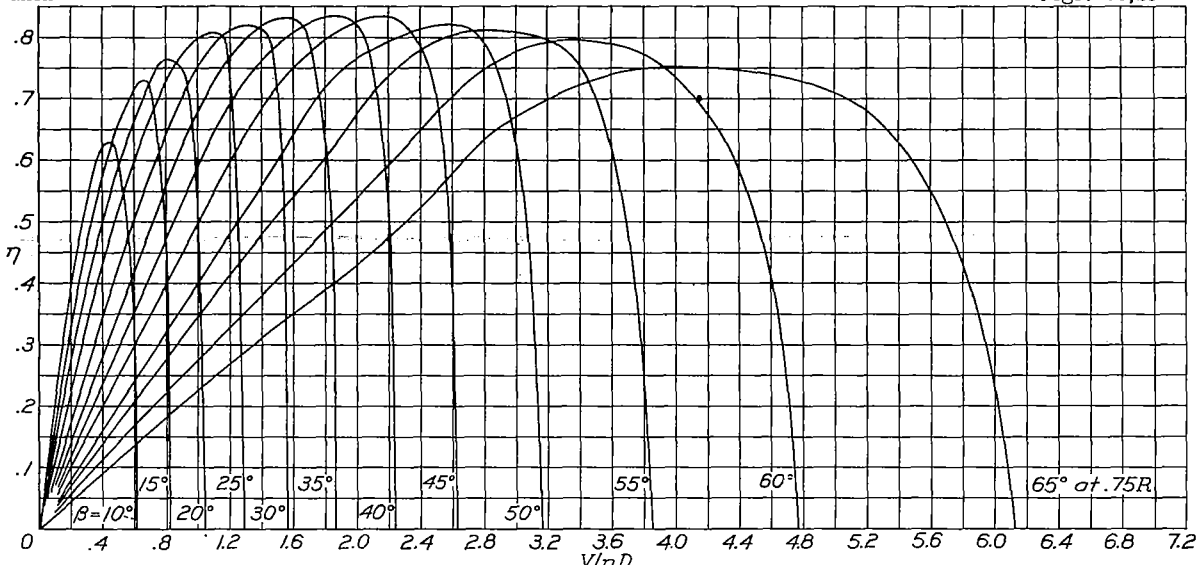


Figure 24.- Efficiency curves for six-blade single-rotating propeller.

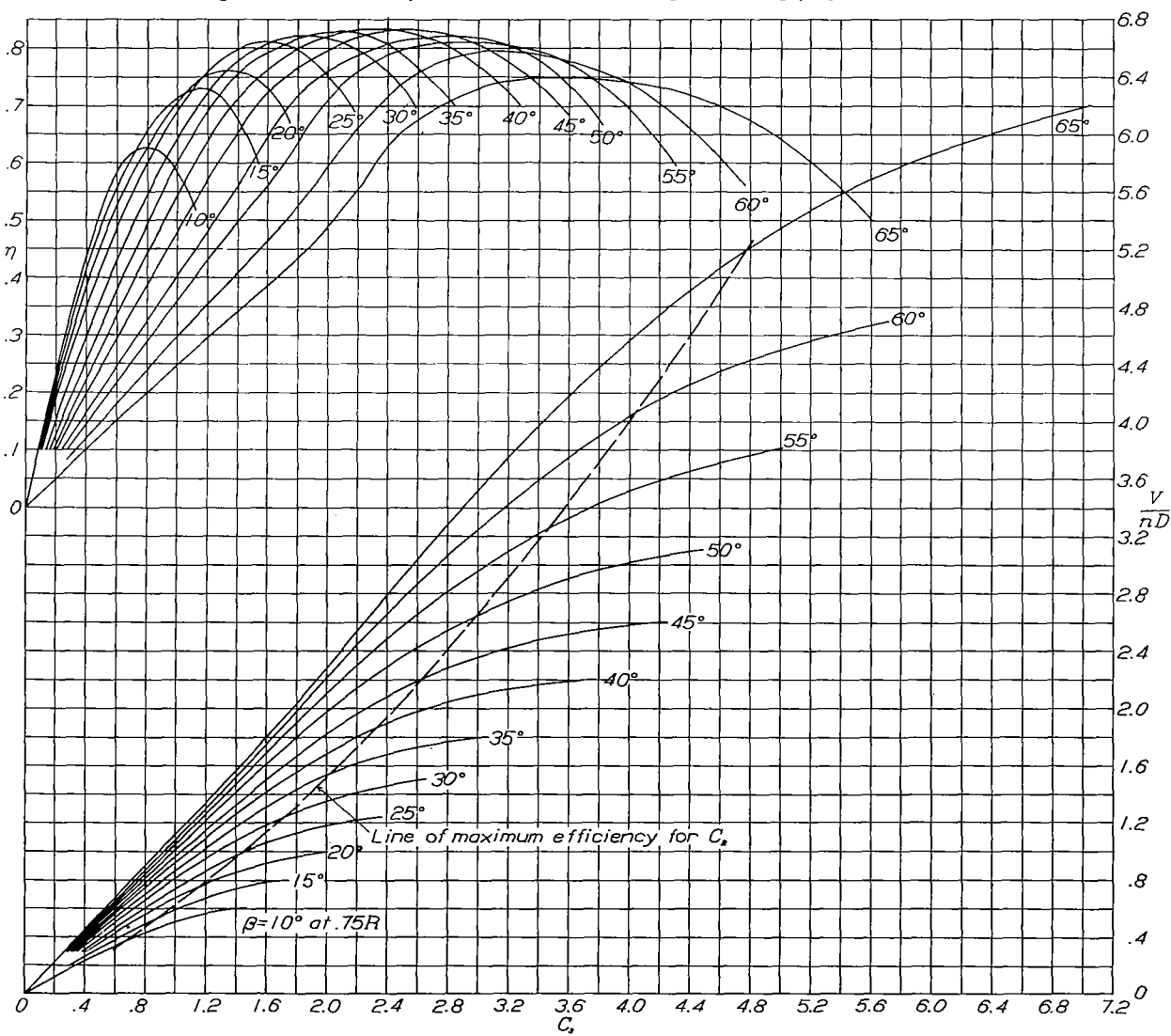


Figure 25.- Design chart for propeller 3155-6-1.5; six blades; single rotation.

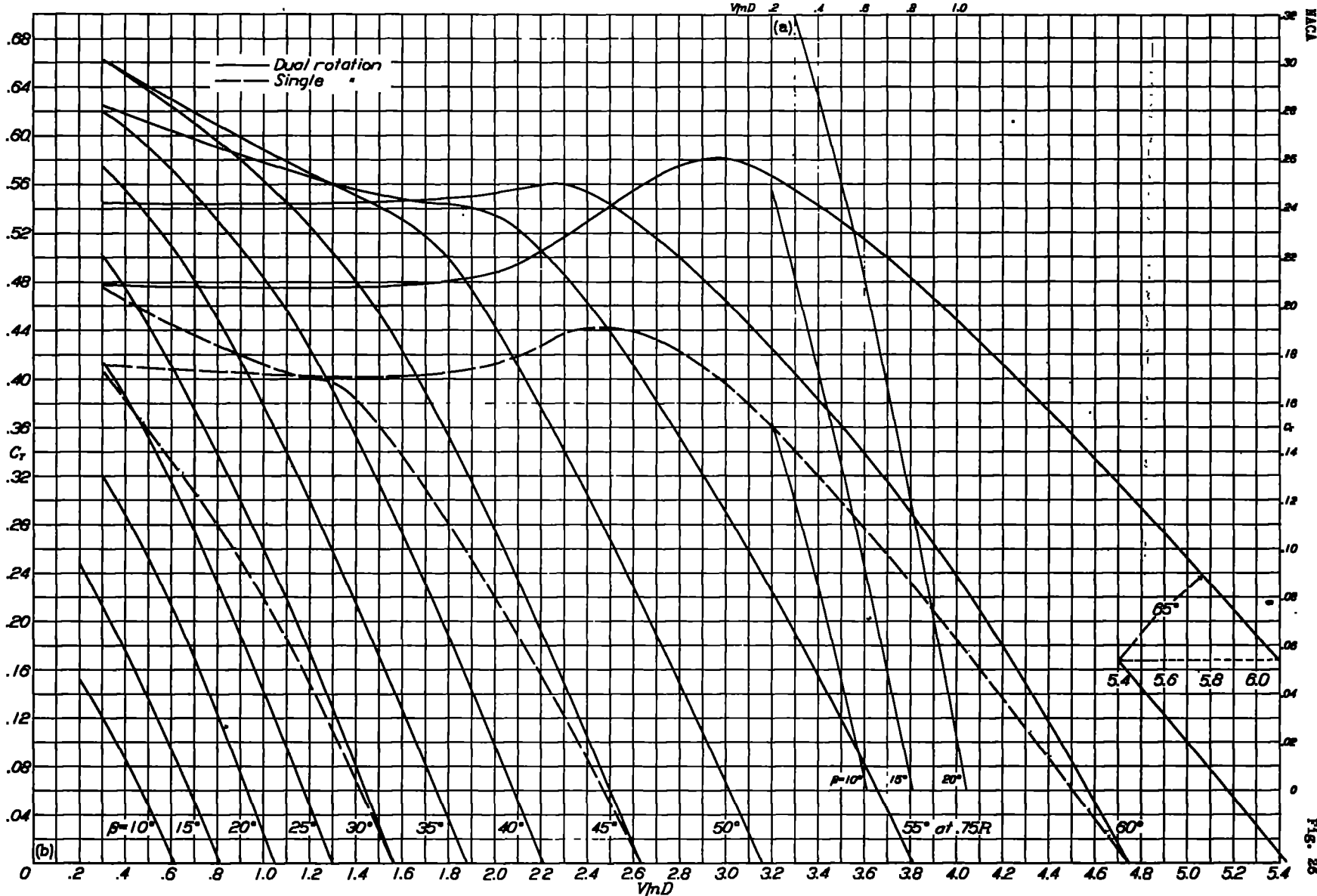


Figure 26.- Thrust-coefficient curves for six-blade dual-rotating propeller, showing superimposed curves for 30°, 45°, and 60° single rotation.

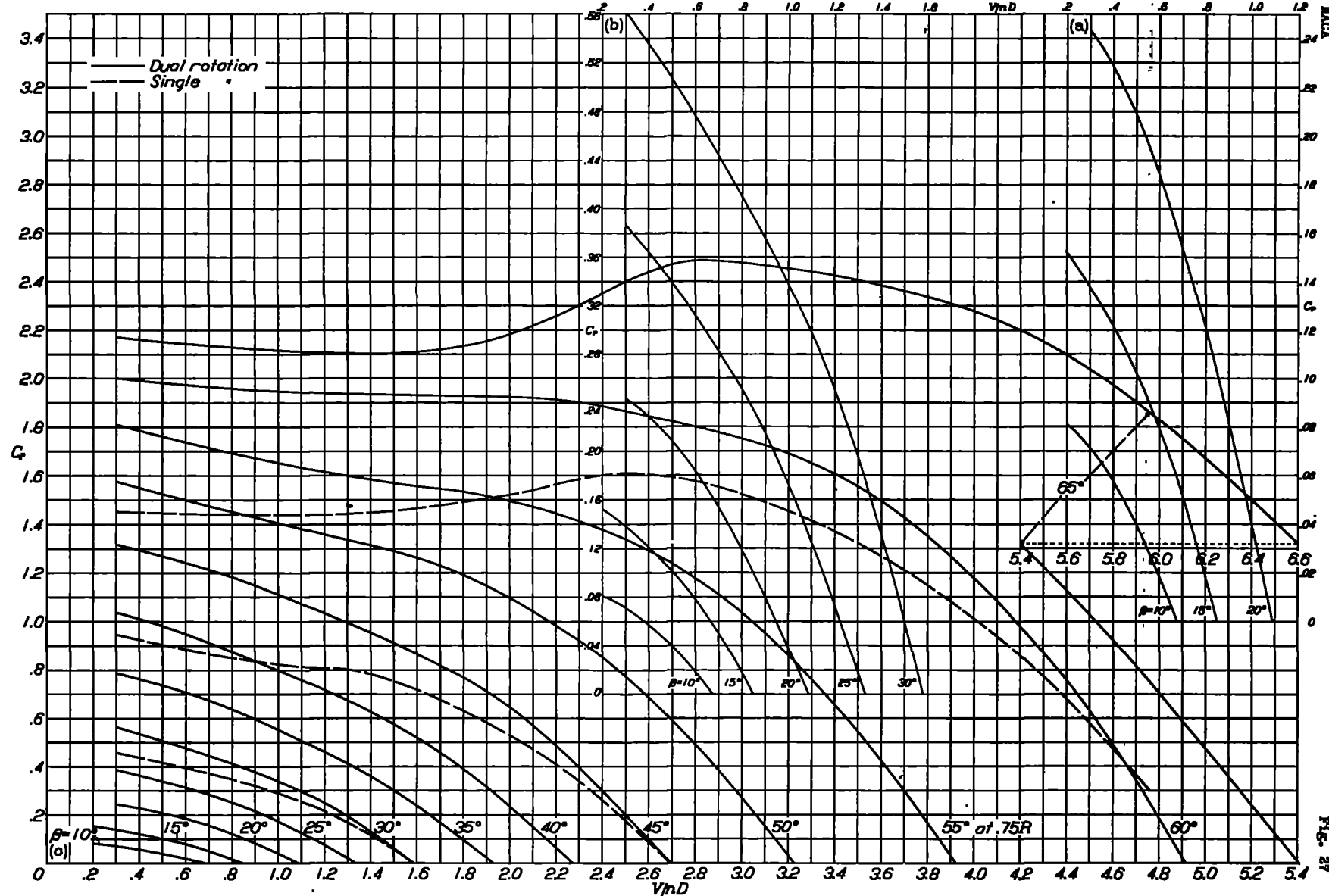


Figure 27.- Power-coefficient curves for six-blade dual-rotating propeller, showing superimposed curves for 30° , 45° , and 60° single rotation.

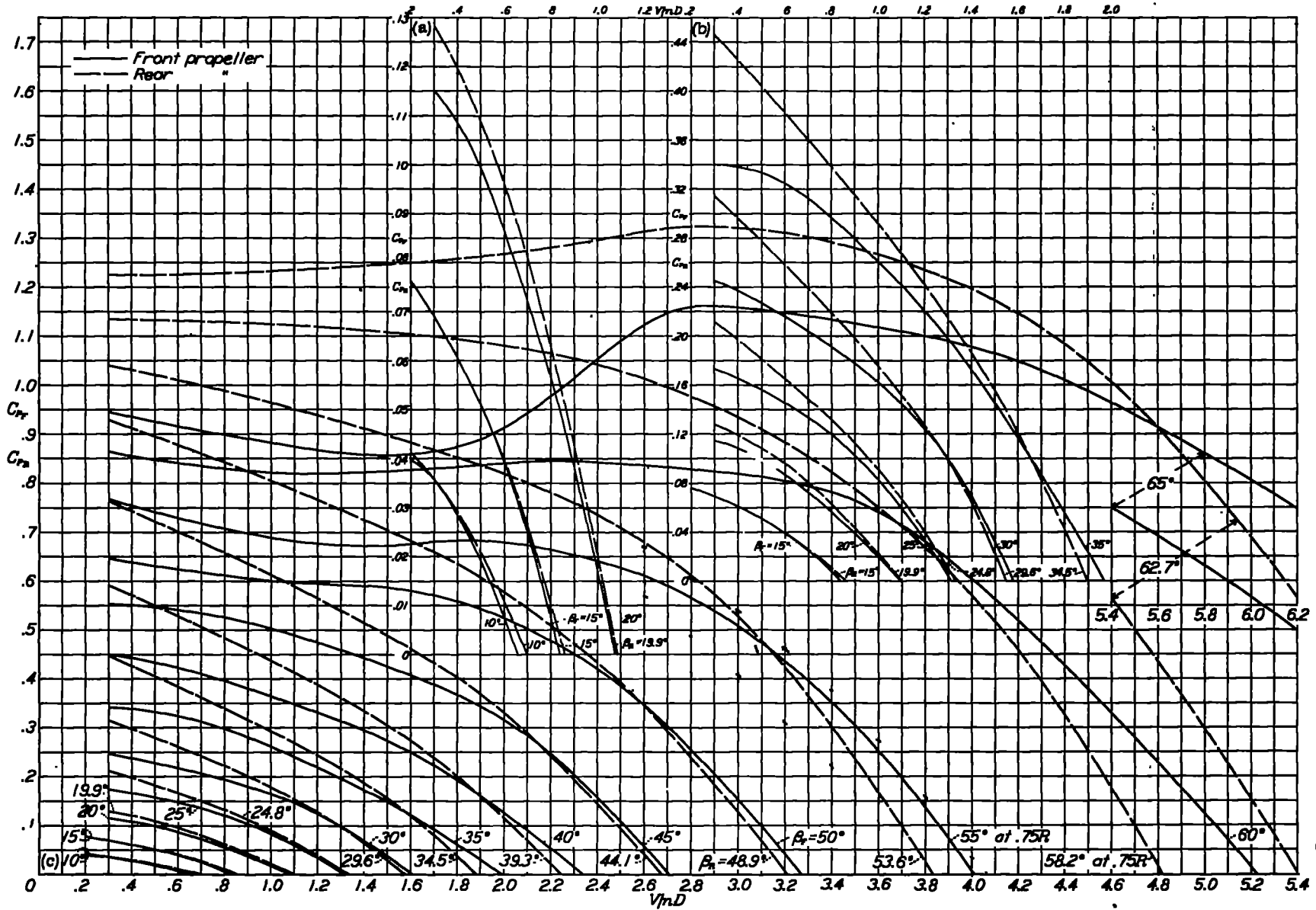


Figure 28.- Individual power-coefficient curves for six-blade dual-rotating propeller.

MACA

Figs. 29,30

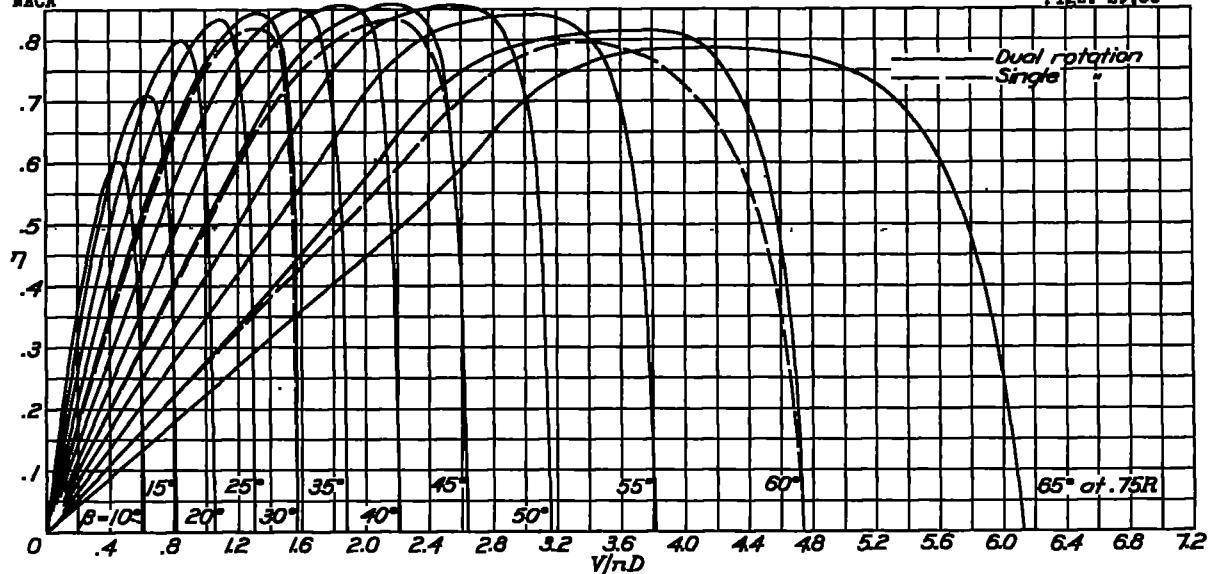


Figure 29.- Efficiency curves for six-blade dual-rotating propeller, showing superimposed curves for $30^\circ, 45^\circ$, and 60° single rotation.

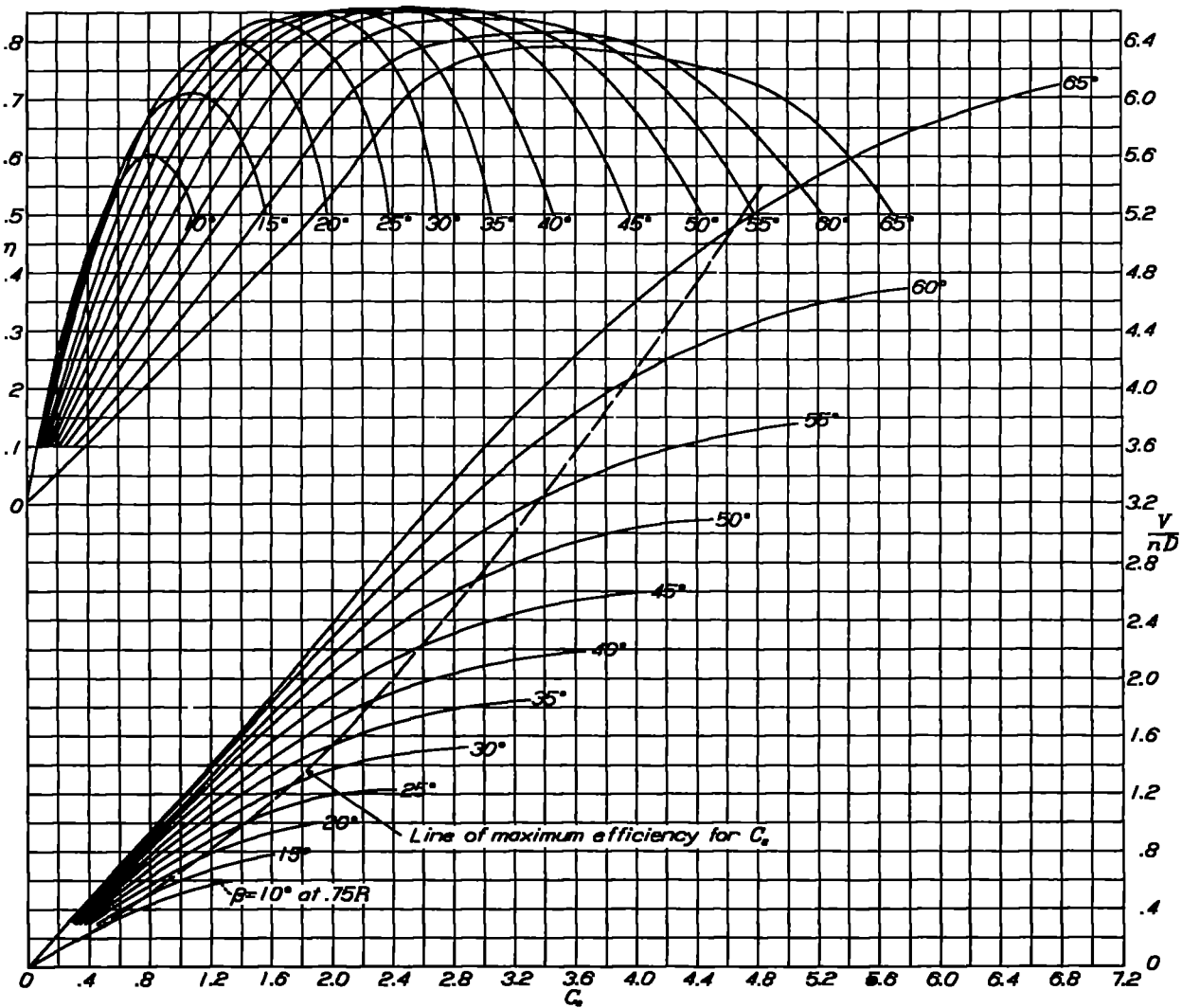


Figure 30.- Design chart for propellers 3155-6-1.5 (R.H.) and 3156-6-1.5 (L.H.); six blade; dual rotation.

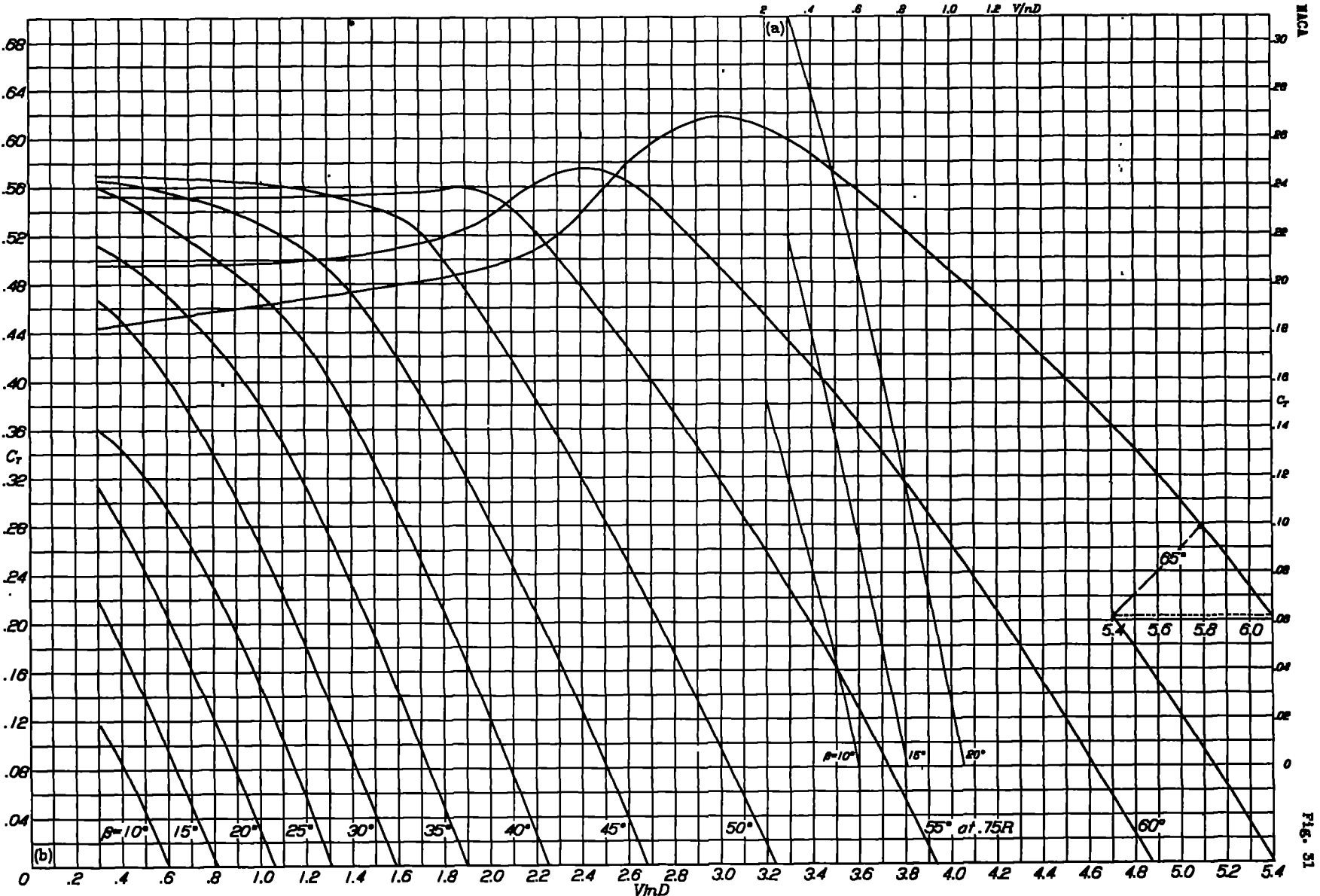


Figure 31.- Thrust-coefficient curves for eight-blade single-rotating propeller.

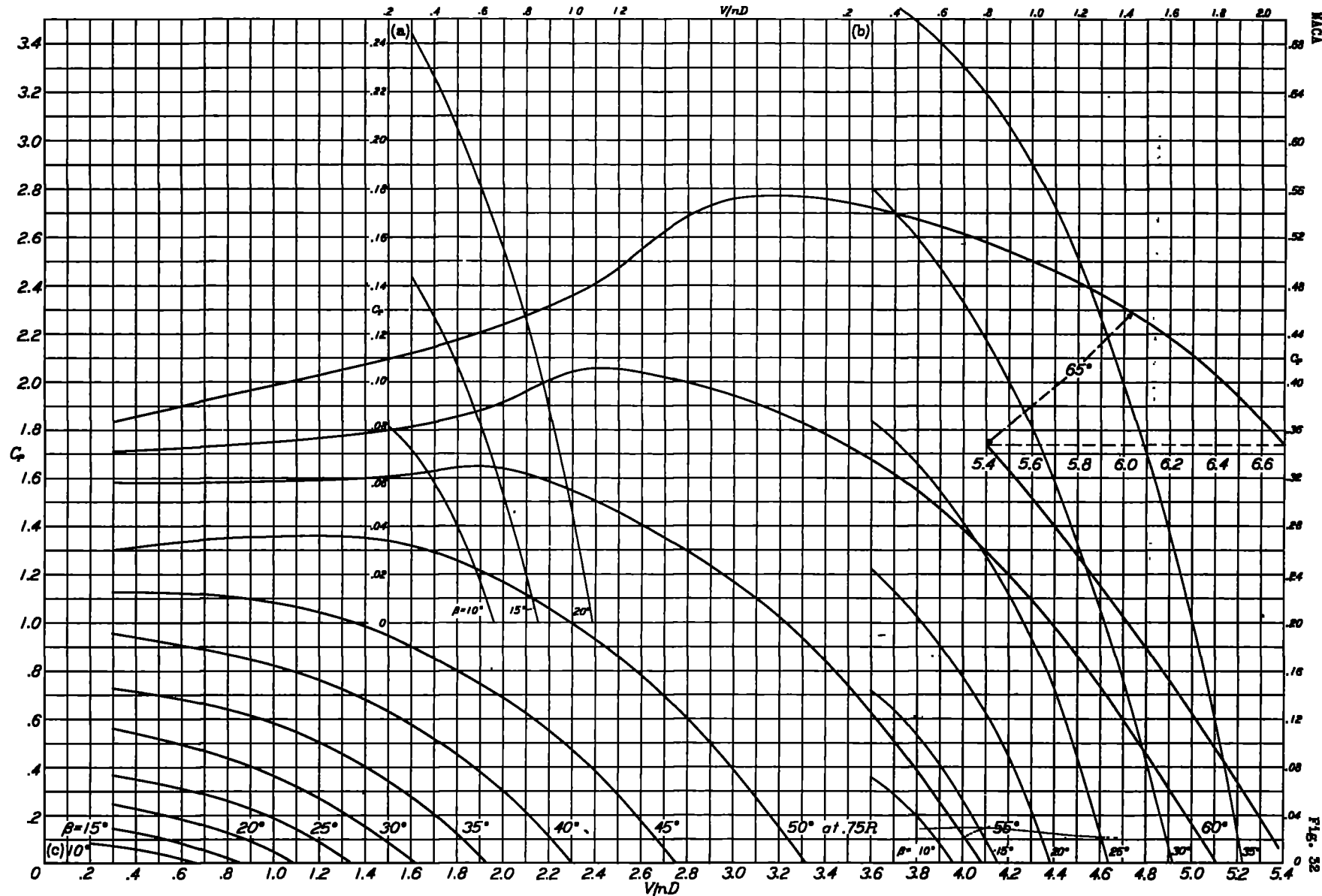


Figure 32.- Power-coefficient curves for eight-blade single-rotating propeller.

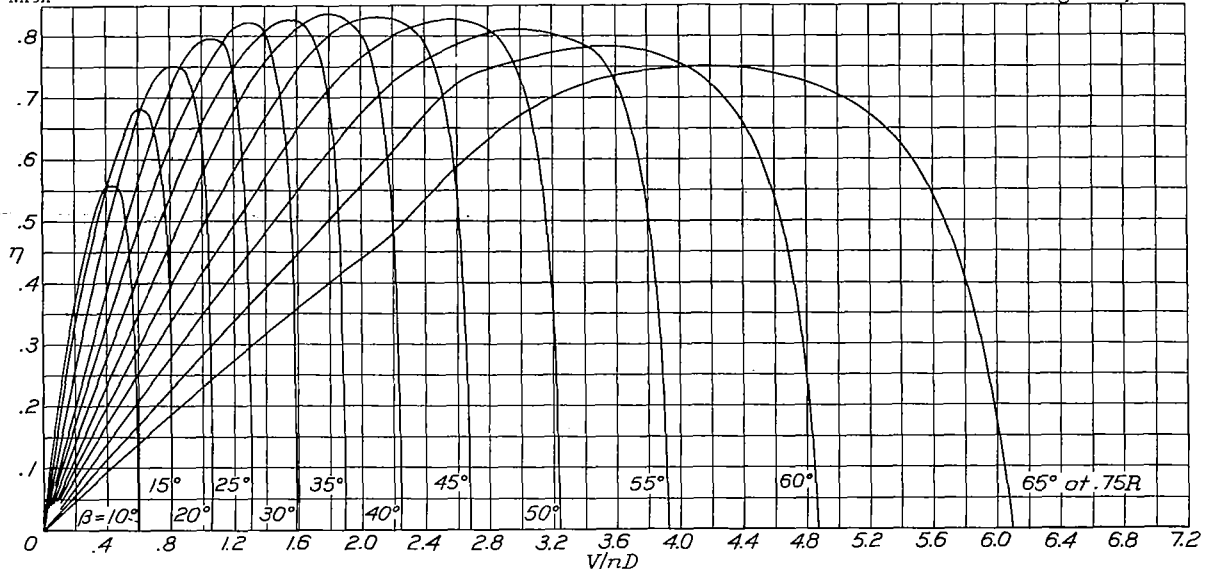


Figure 33.- Efficiency curves for eight-blade single-rotating propeller.

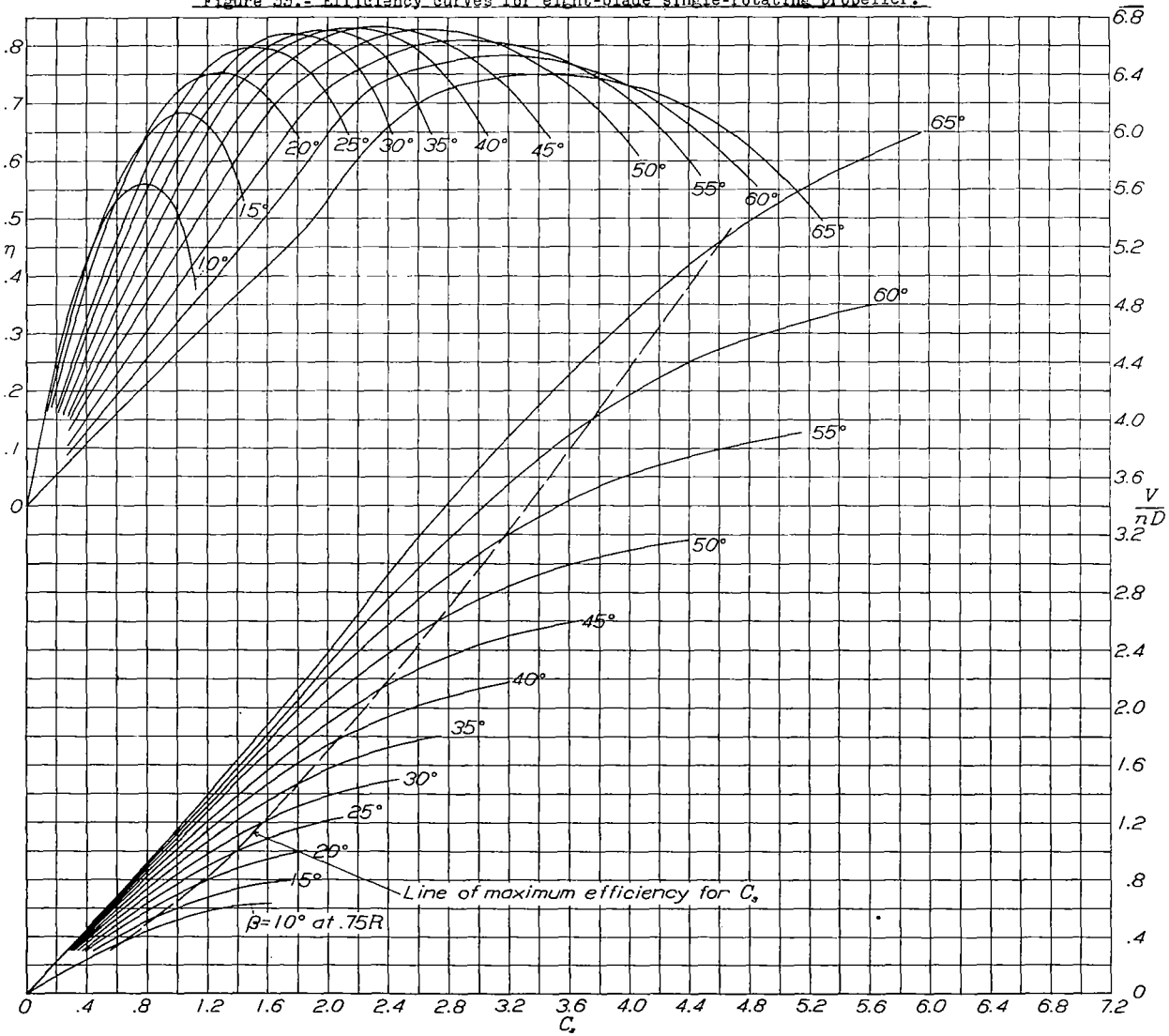


Figure 34.- Design chart for propeller 3155-6-1.5; eight blade; single rotation.

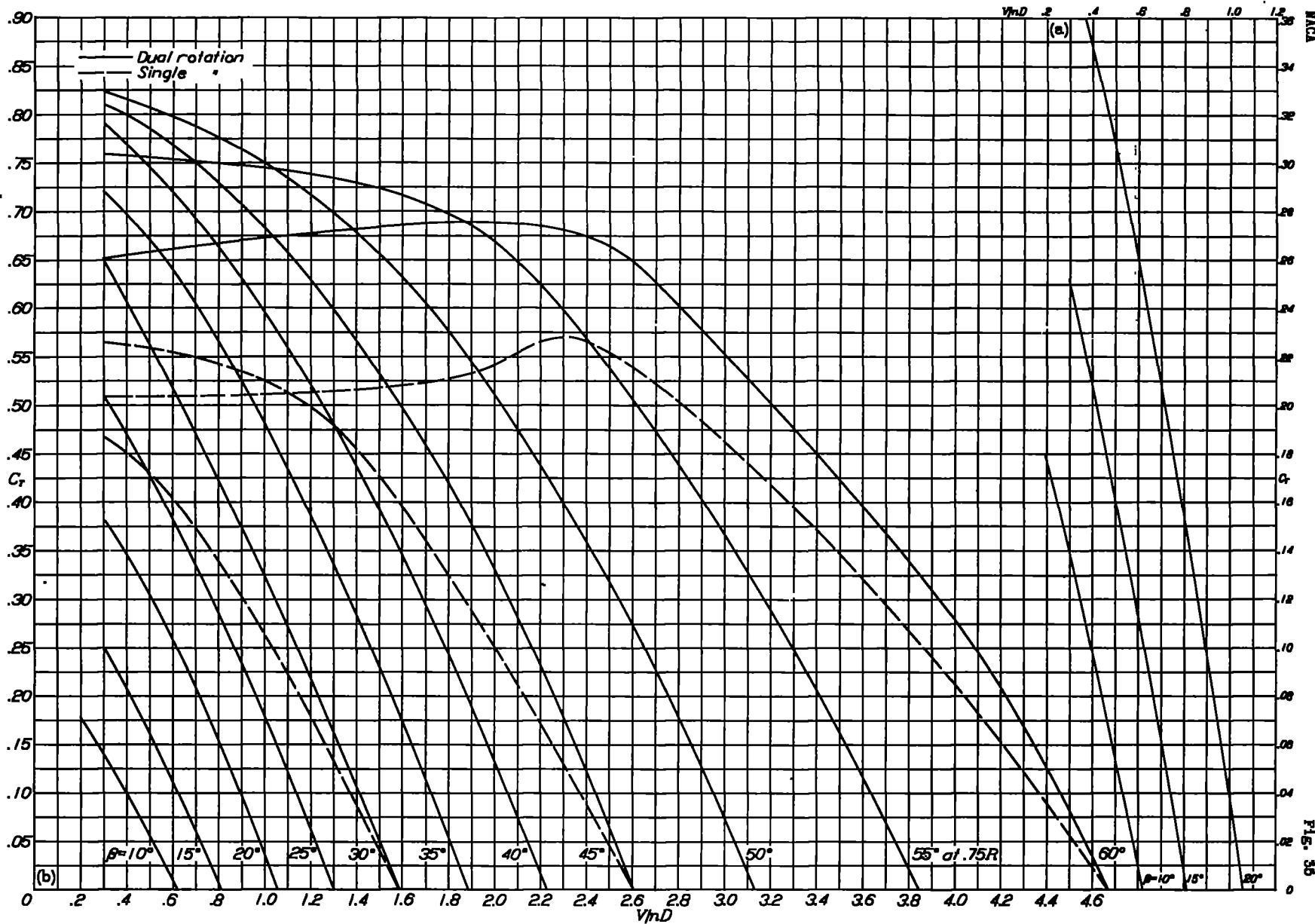


Figure 35b.- Thrust-coefficient curves for eight-blade dual-rotating propeller, showing superimposed curves for 30° , 45° , and 60° single rotation.

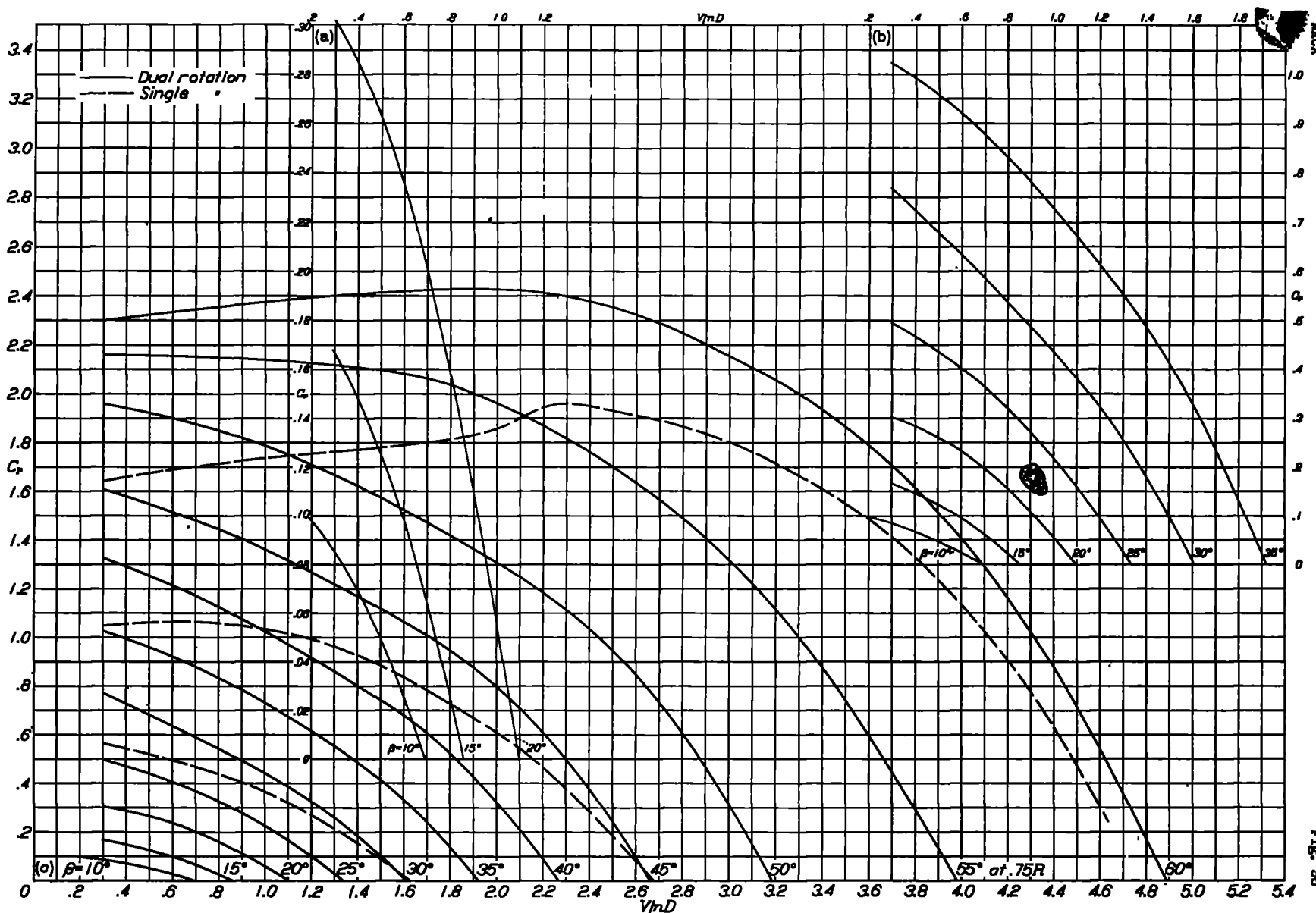


Figure 36.- Power-coefficient curves for eight-blade dual-rotating propeller, showing superimposed curves for 30° , 45° , and 60° single rotation.

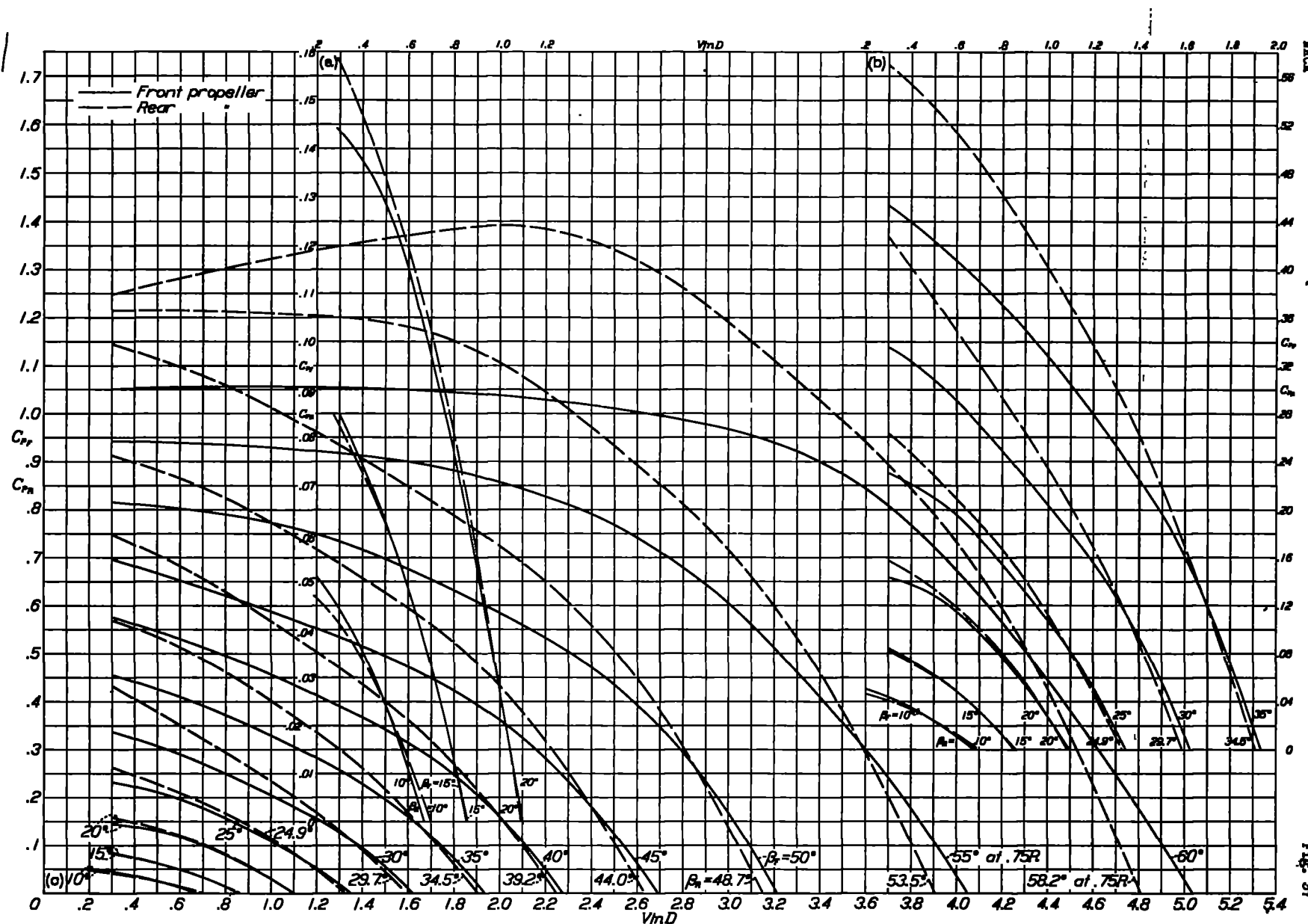


Figure 37.- Individual power-coefficient curves for eight-blade dual-rotating propeller.

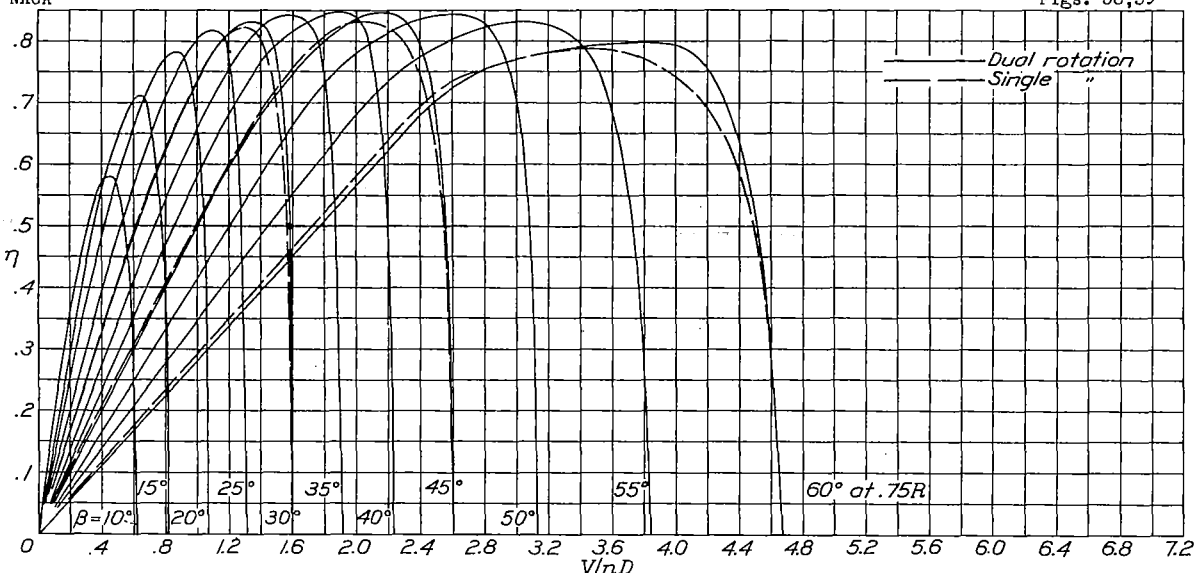


Figure 38.- Efficiency curves for eight-blade dual-rotating propeller, showing superimposed curves for 30° , 45° , and 60° single rotation.

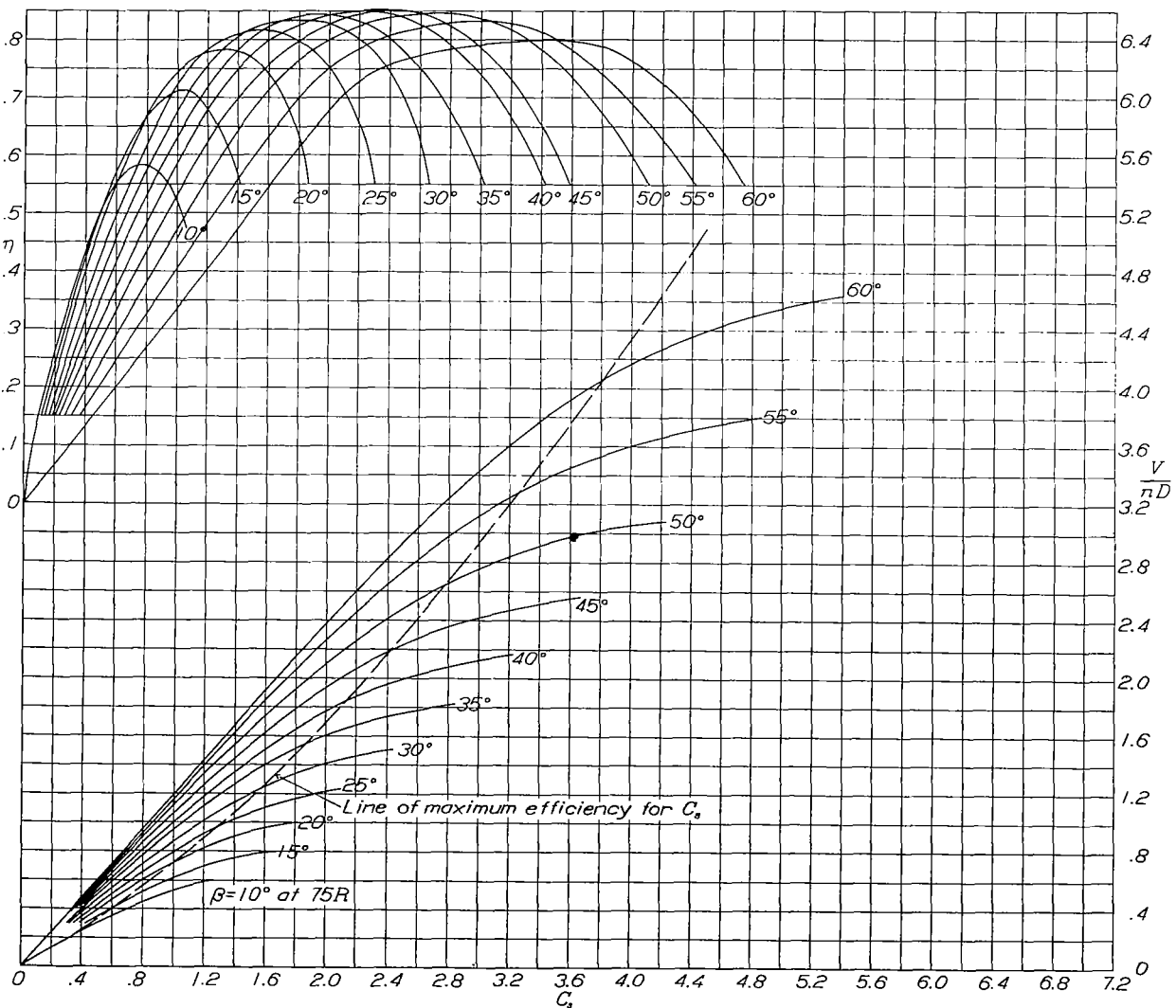


Figure 39.- Design chart for propellers 3155-6-1.5 (R.H.) and 3156-6-1.5 (L.H.); eight blade; dual rotation.

NACA

Fig. 40

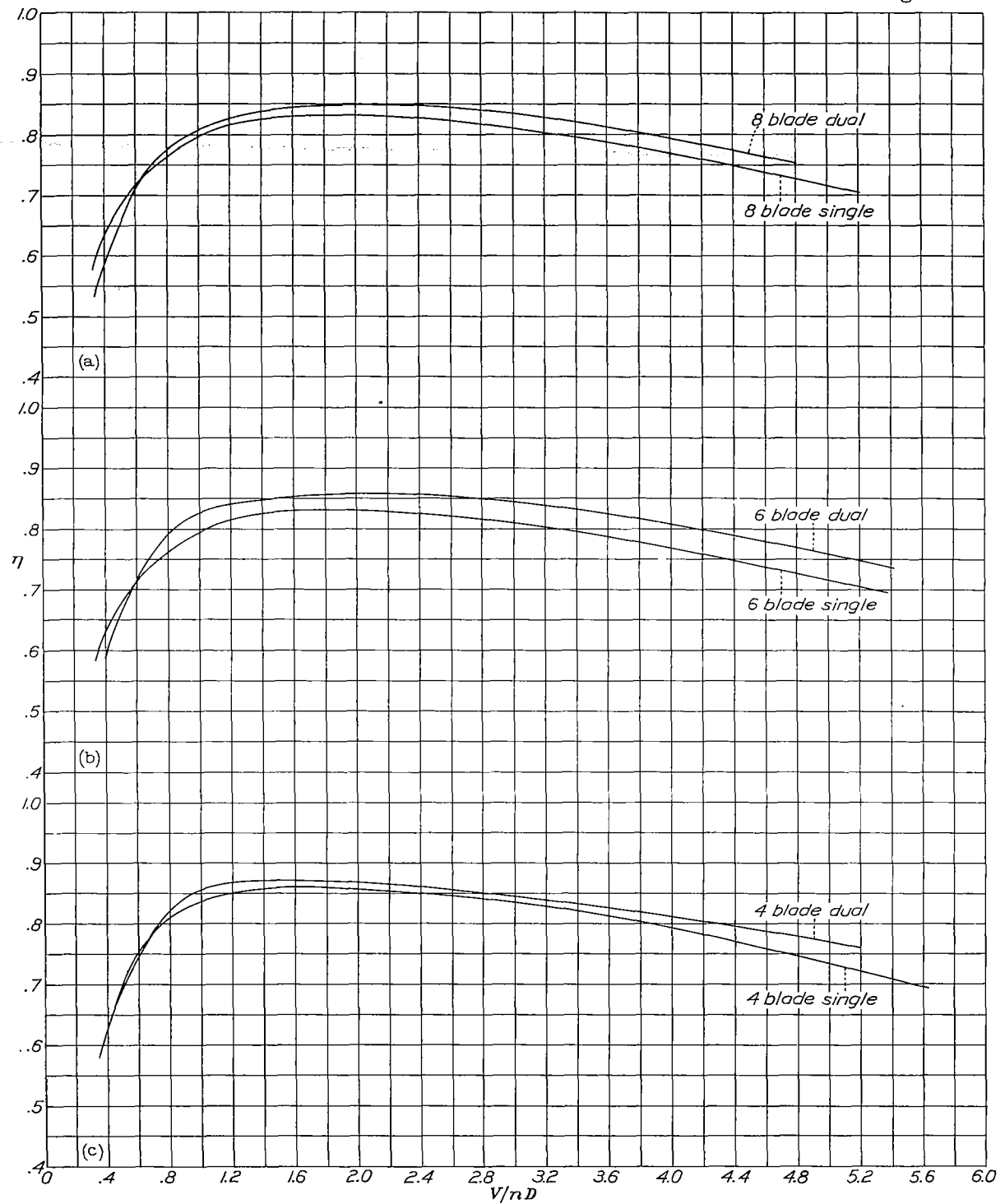


Figure 40.- Effect of dual rotation on efficiency envelopes.

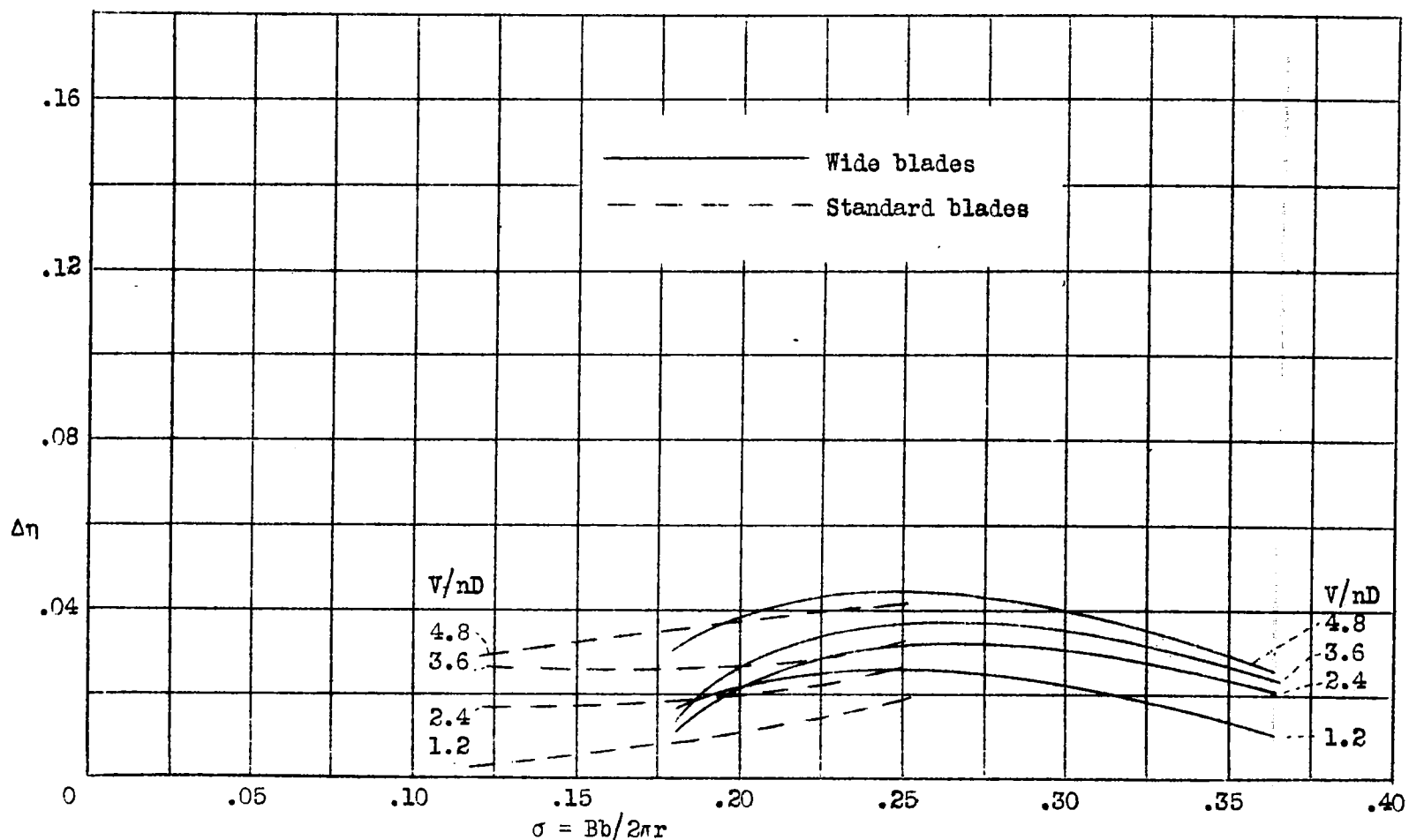
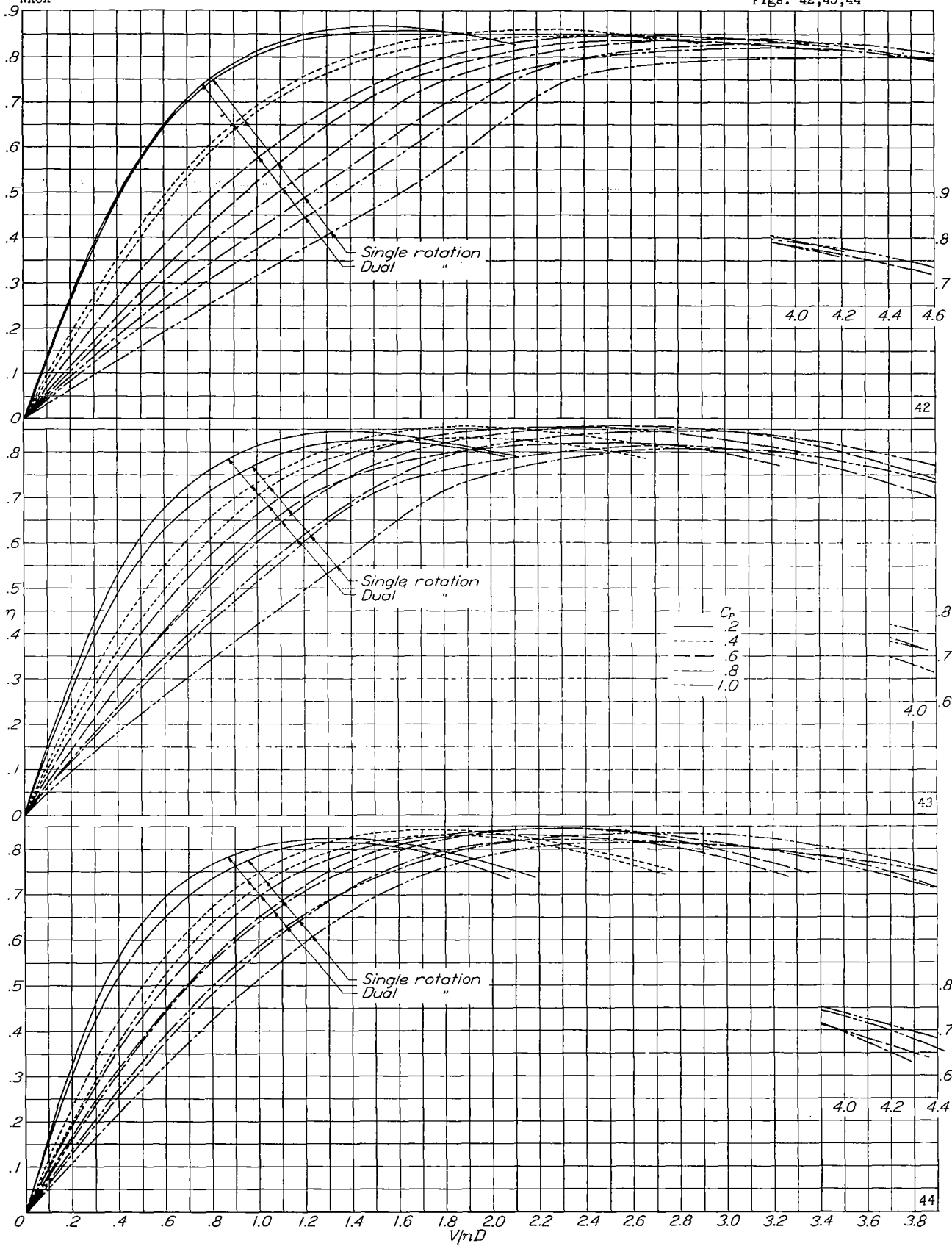


Figure 41.— Variations in the efficiency gain due to dual rotation with solidity and V/nD . With wing.



(42) Four-blade propeller

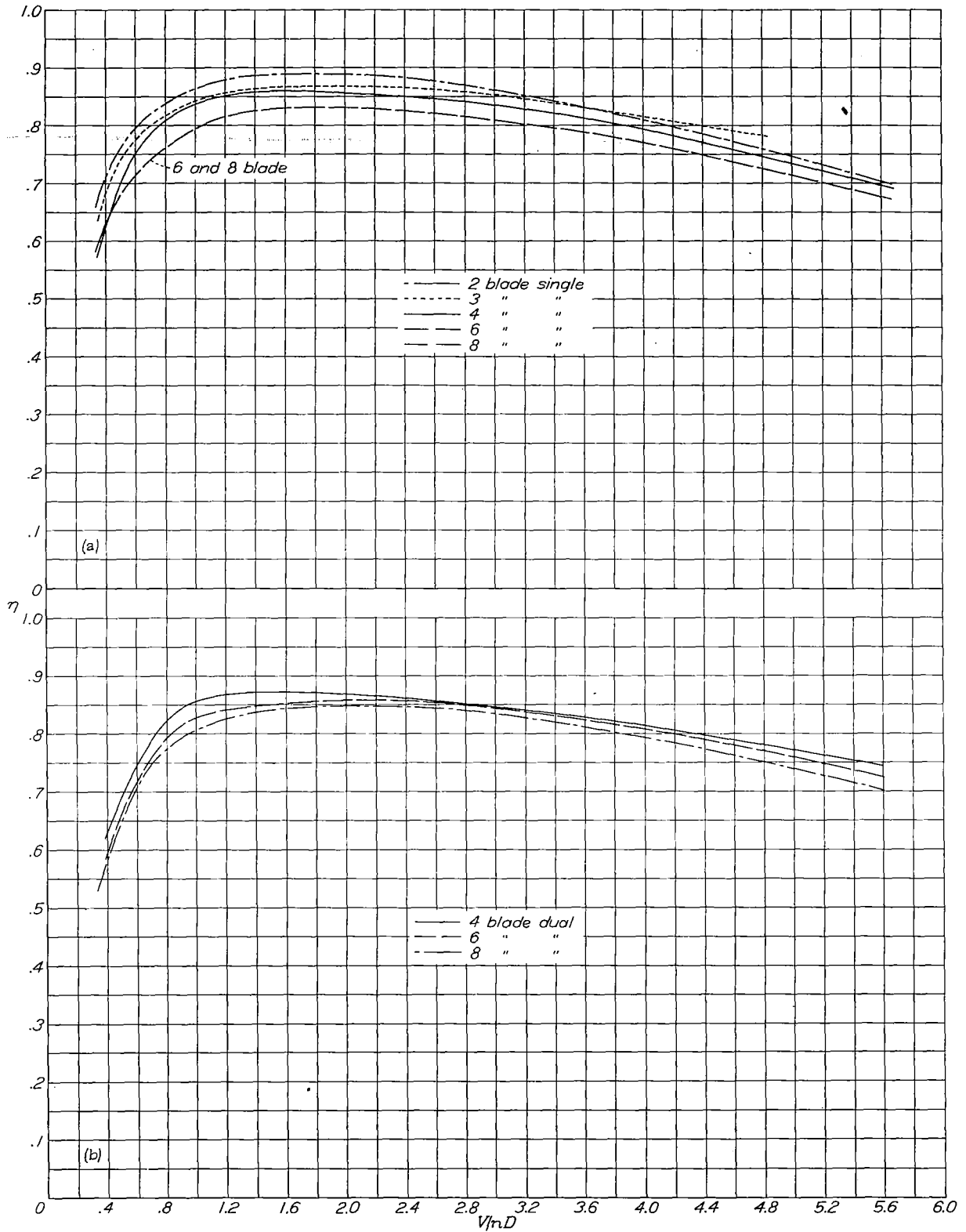
(43) Six-blade propeller

(44) Eight-blade propeller

Figures 42, 43, and 44.- Effect of dual rotation on efficiency for propellers at constant power.

NACA

Fig. 45



(a) Single rotation

(b) Dual rotation

Figure 45.- Efficiency envelope comparisons for different solidities.

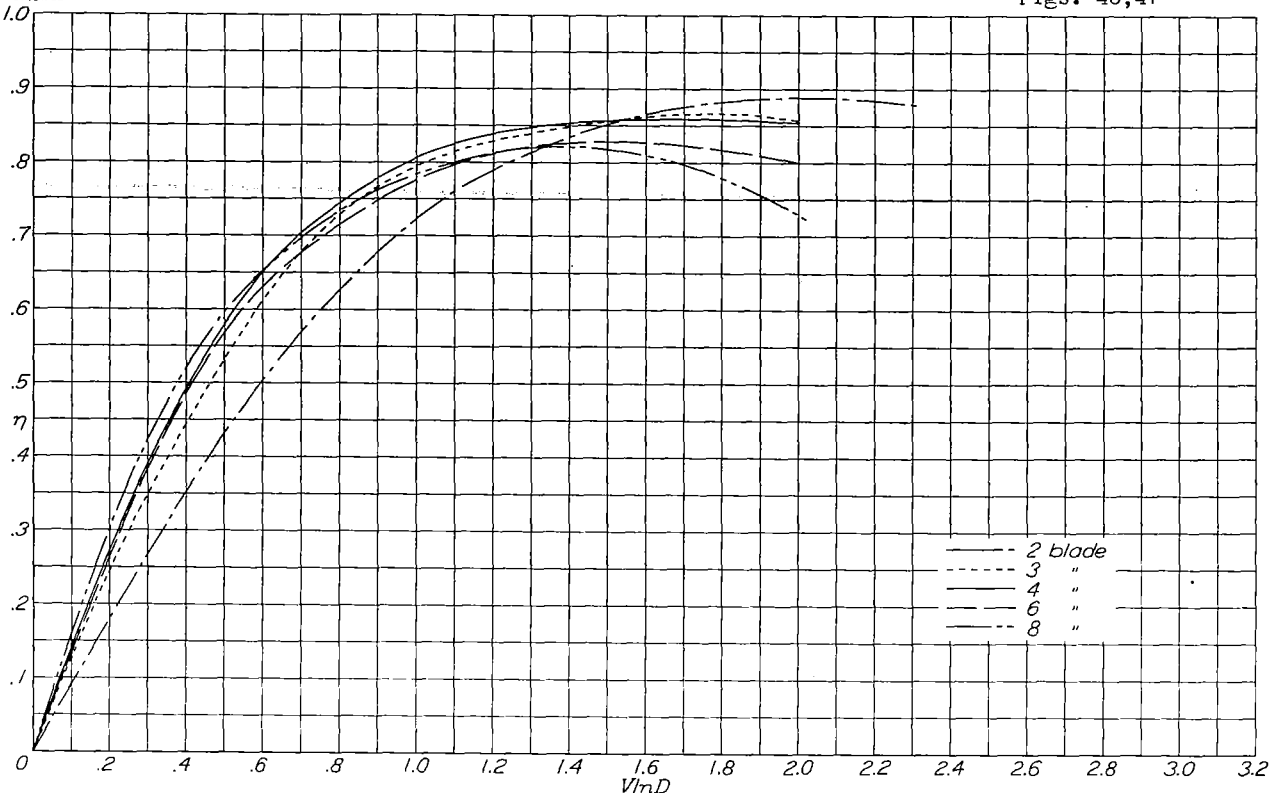


Figure 46.- Effect of solidity on efficiency for single rotation at constant C_p of 0.2.

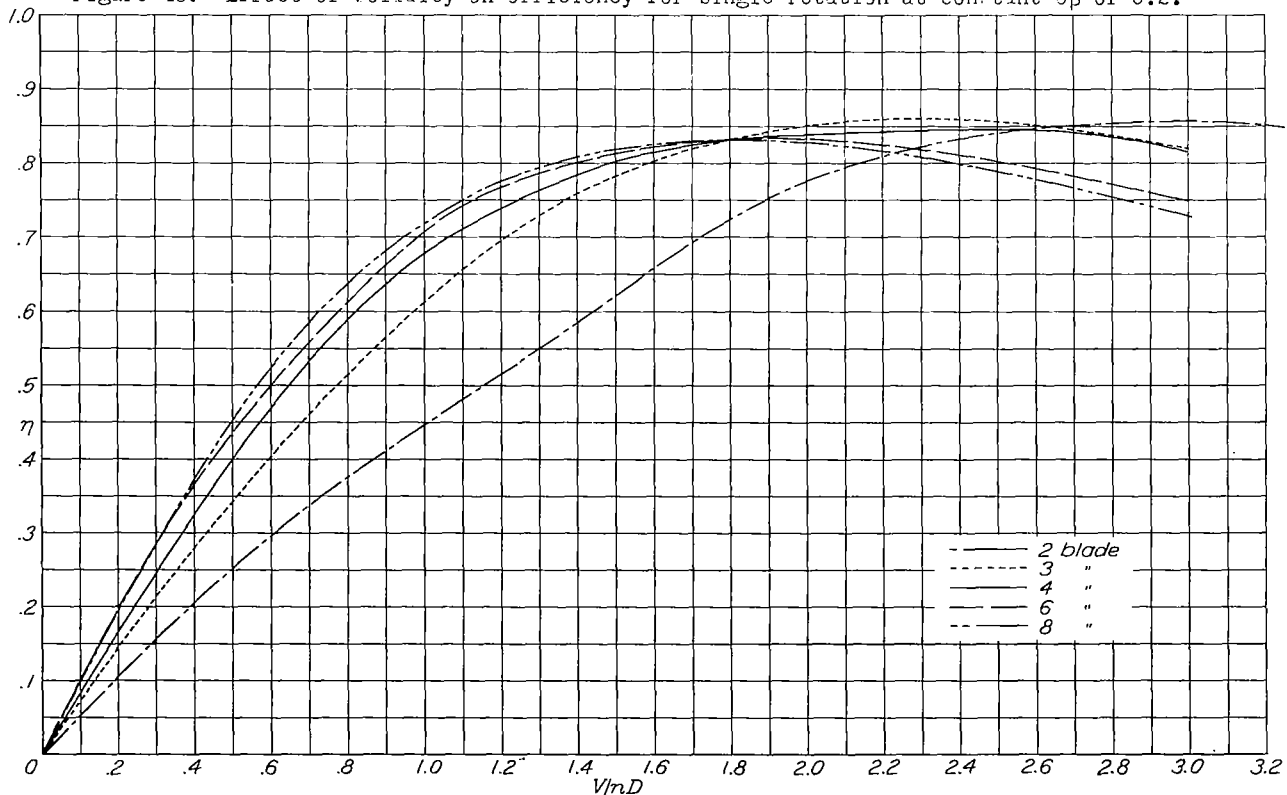
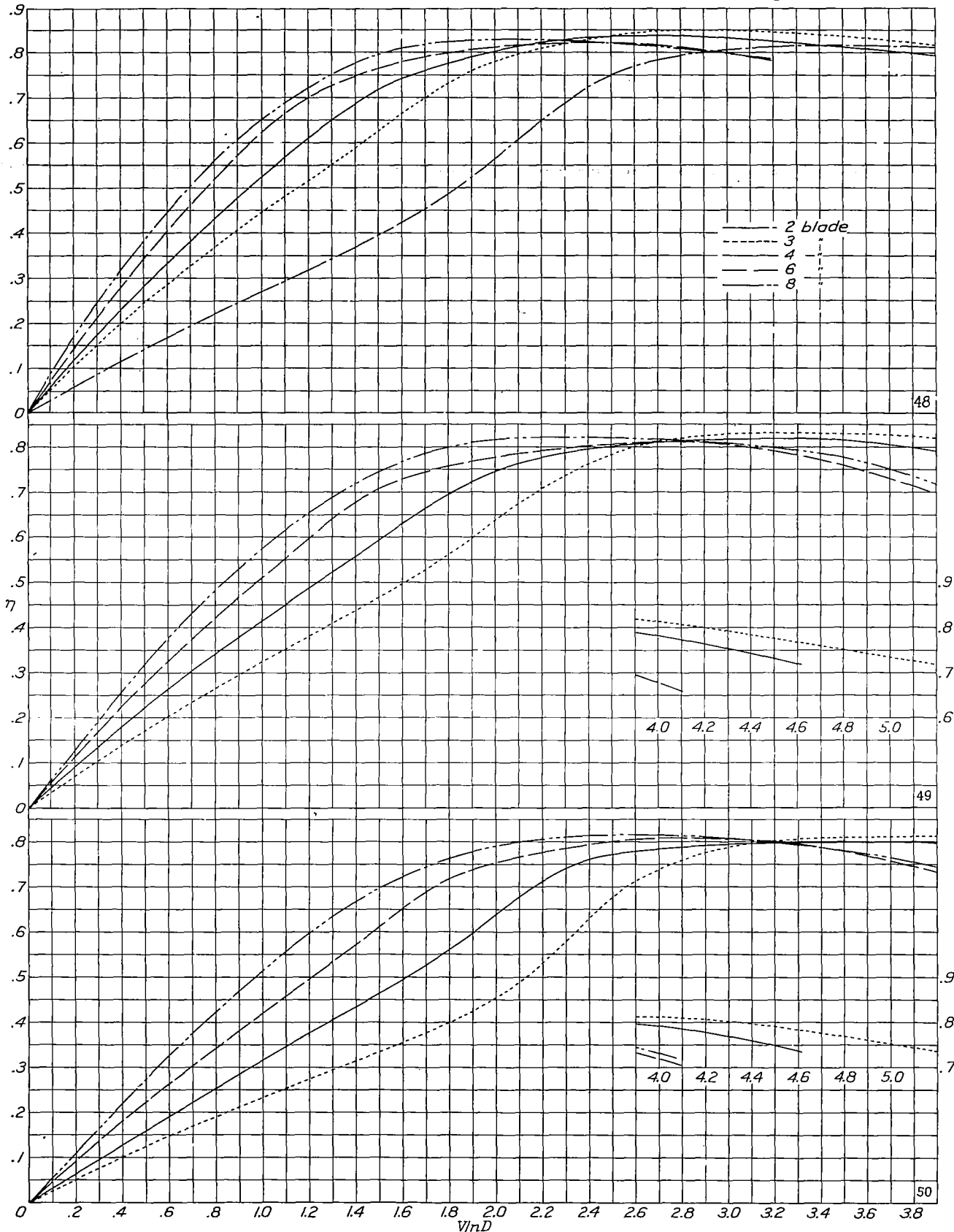


Figure 47.- Effect of solidity on efficiency for single rotation at constant C_p of 0.4.

(48) $C_p = 0.6$ (49) $C_p = 0.8$ (50) $C_p = 1.0$ Figures 48, 49, and 50.- Effect of solidity on efficiency for single rotation at constant C_p .

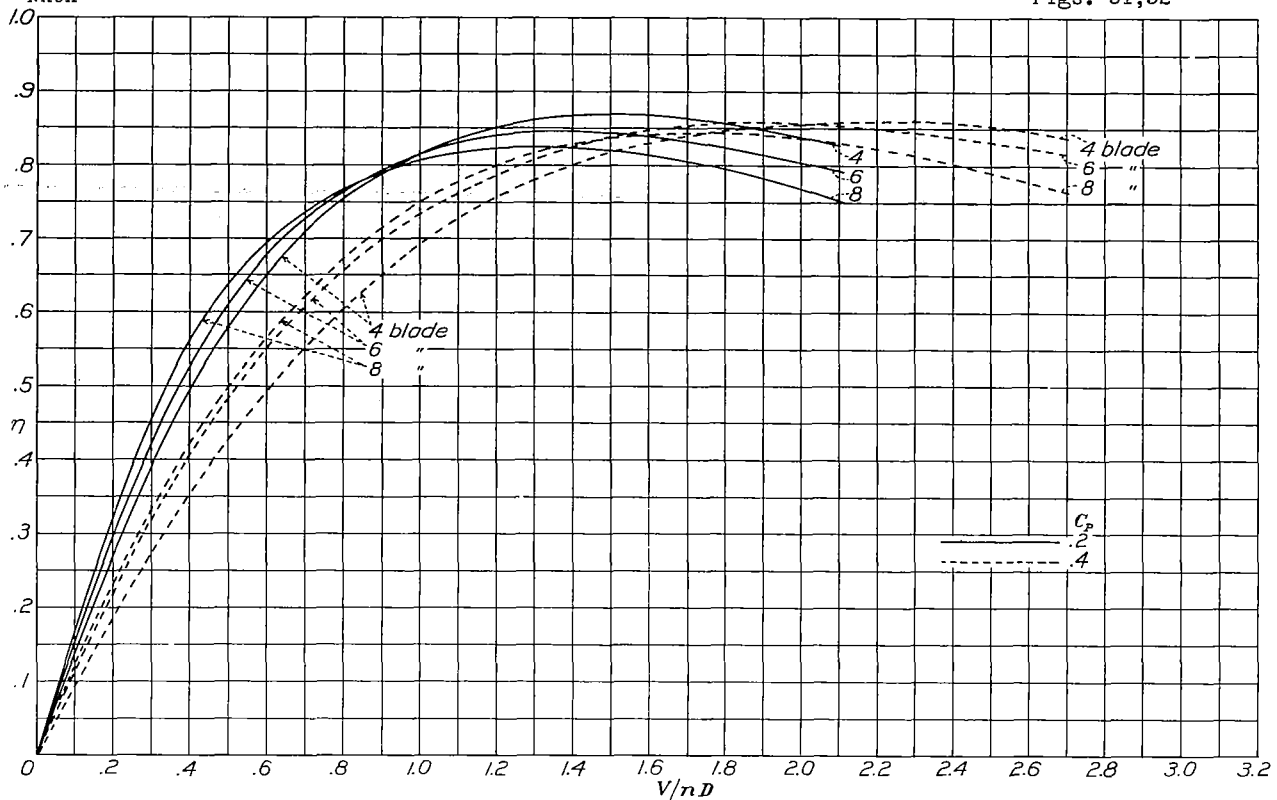


Figure 51.- Effect of solidity on efficiency for dual rotation at constant power.

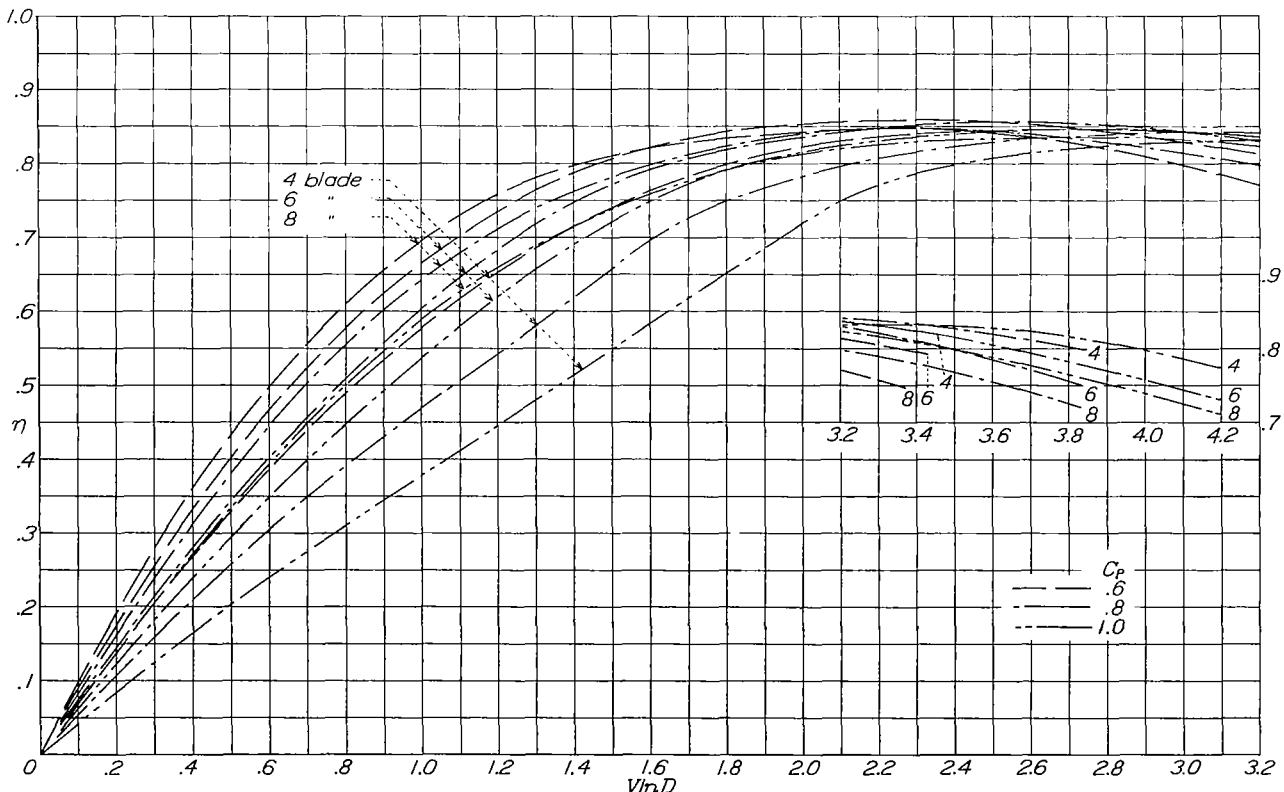
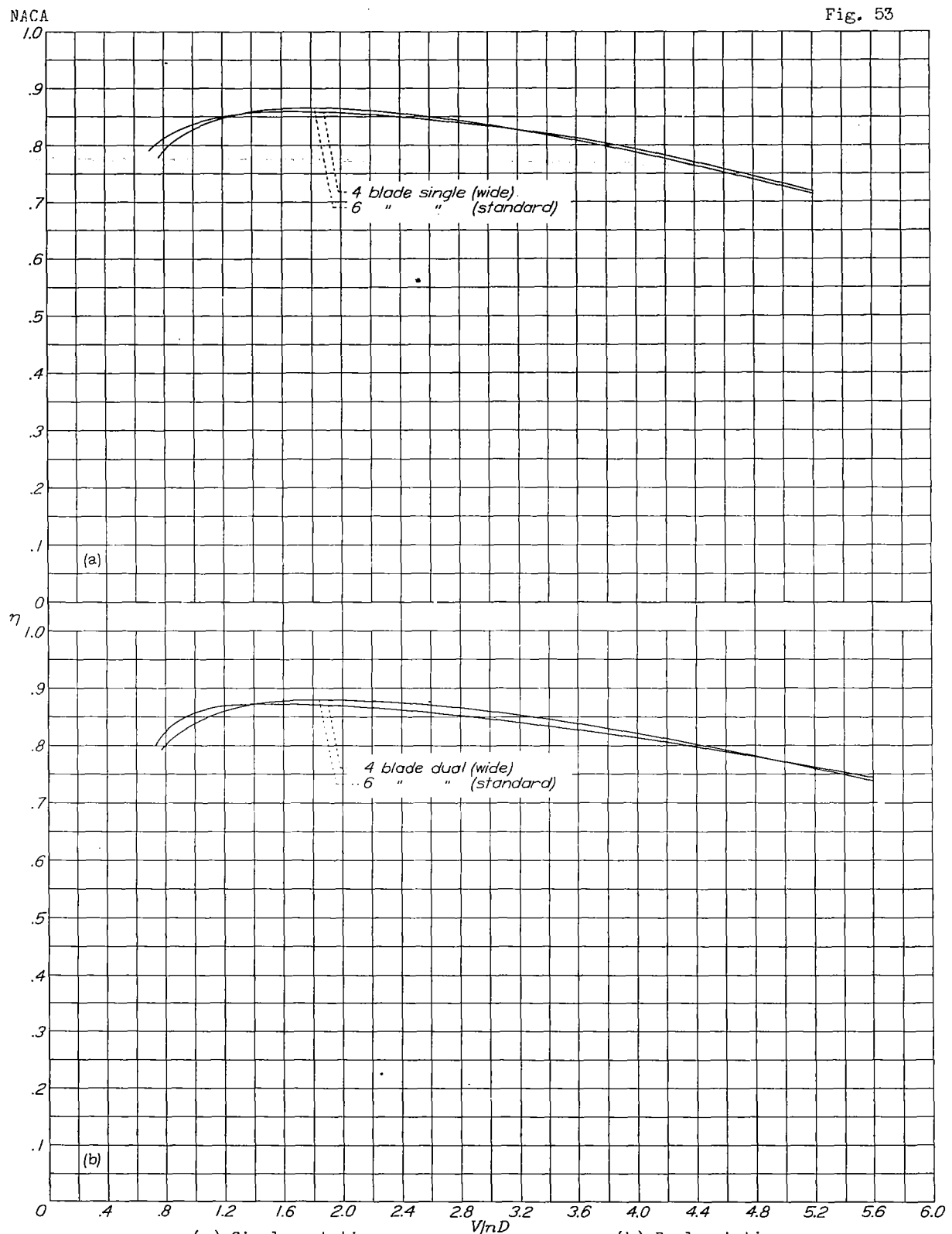


Figure 52.- Effect of solidity on efficiency for dual rotation at constant power.

Fig. 53



(a) Single rotation

(b) Dual rotation

Figure 53.- Efficiency envelopes for propellers having the same solidity but different number of blades.

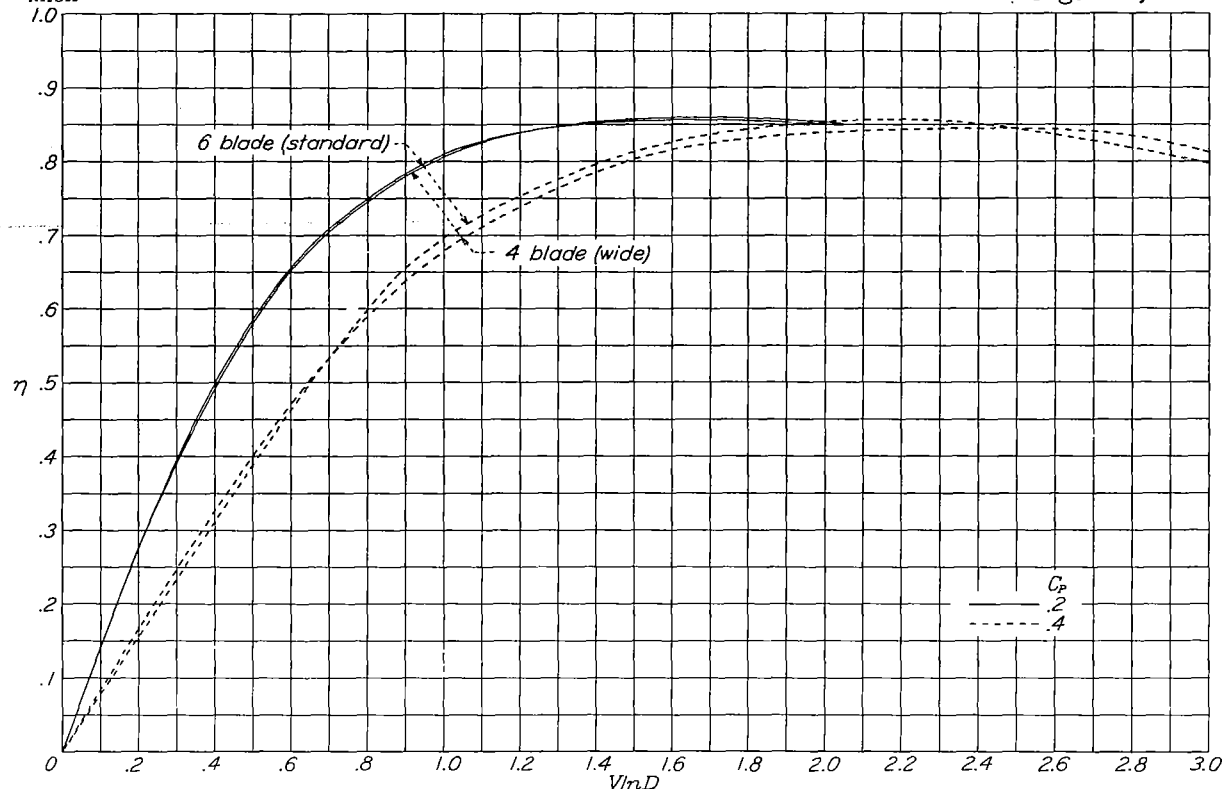


Figure 54.- Comparison of efficiencies at constant power for single rotating propellers having the same solidities but different number of blades.

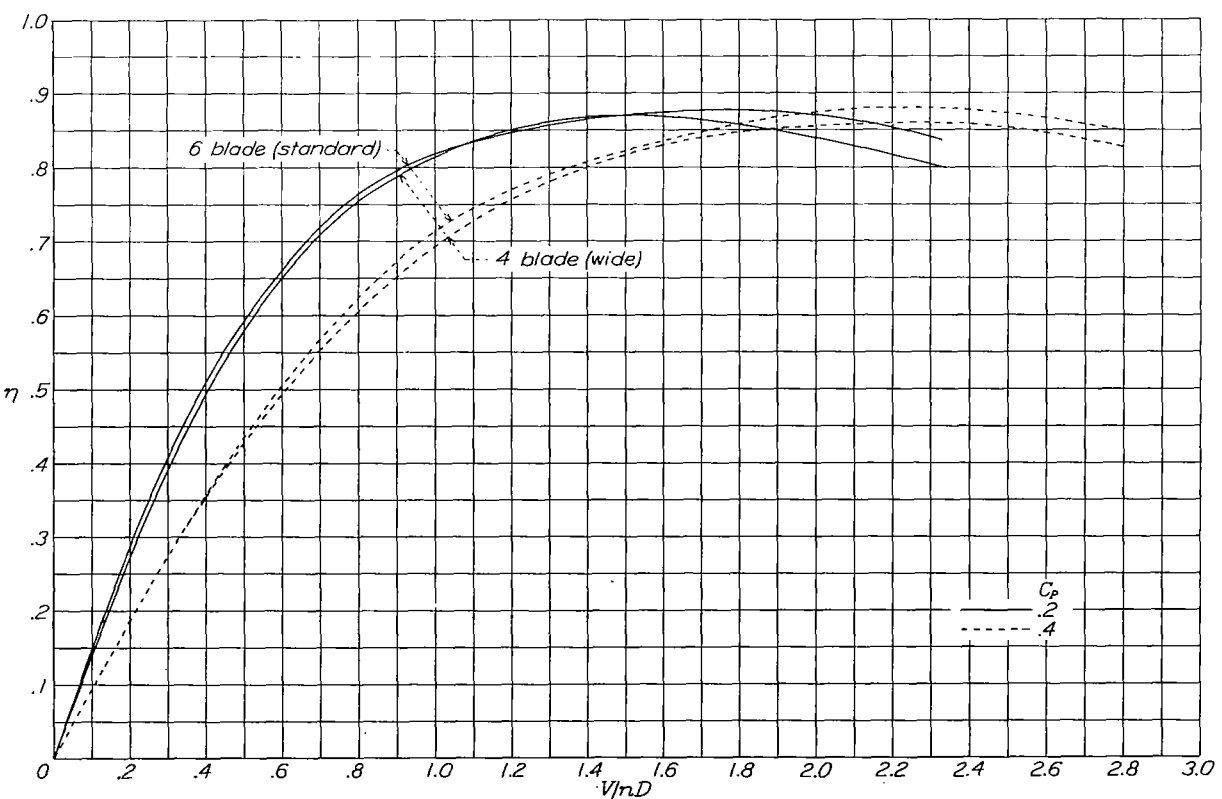


Figure 55.- Comparison of efficiencies at constant power for dual rotating propellers having the same solidities but different number of blades.

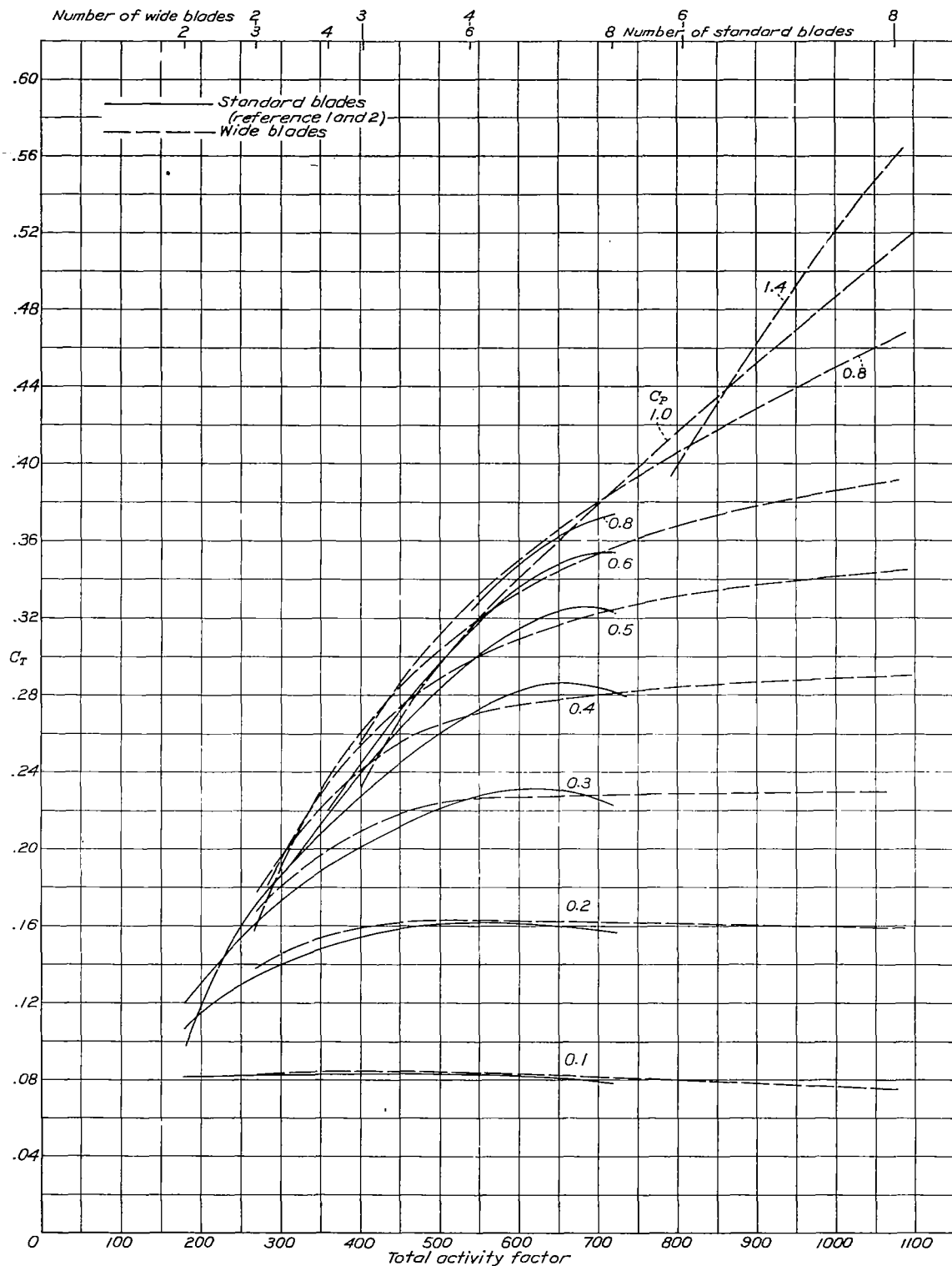


Figure 56.- Variation of thrust coefficient with activity factor.
 $V/nD = 1.0$.

NACA

Fig. 57

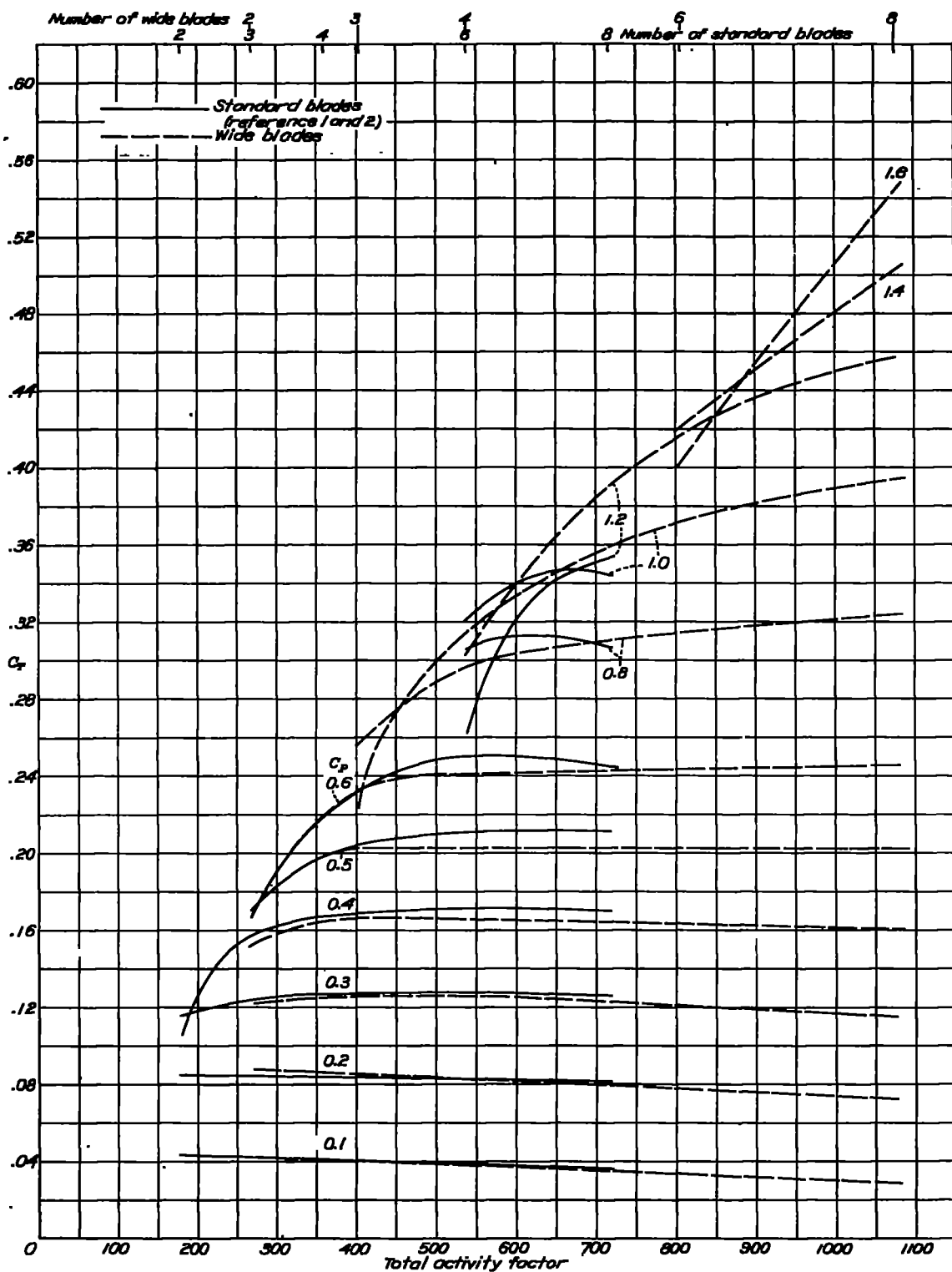


Figure 57.- Variation of thrust coefficient with activity factor.
 $V/nD = 2.0$.

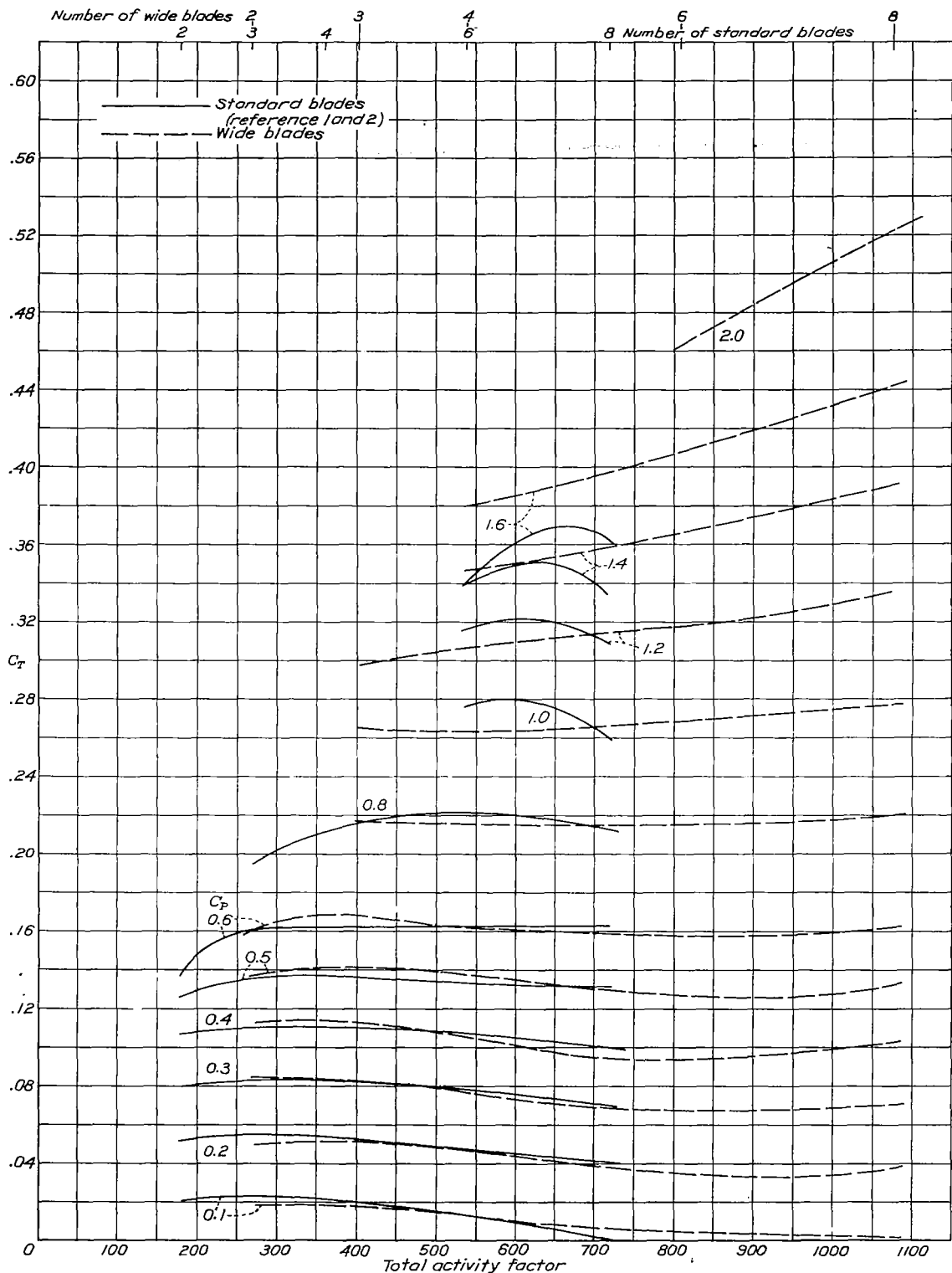
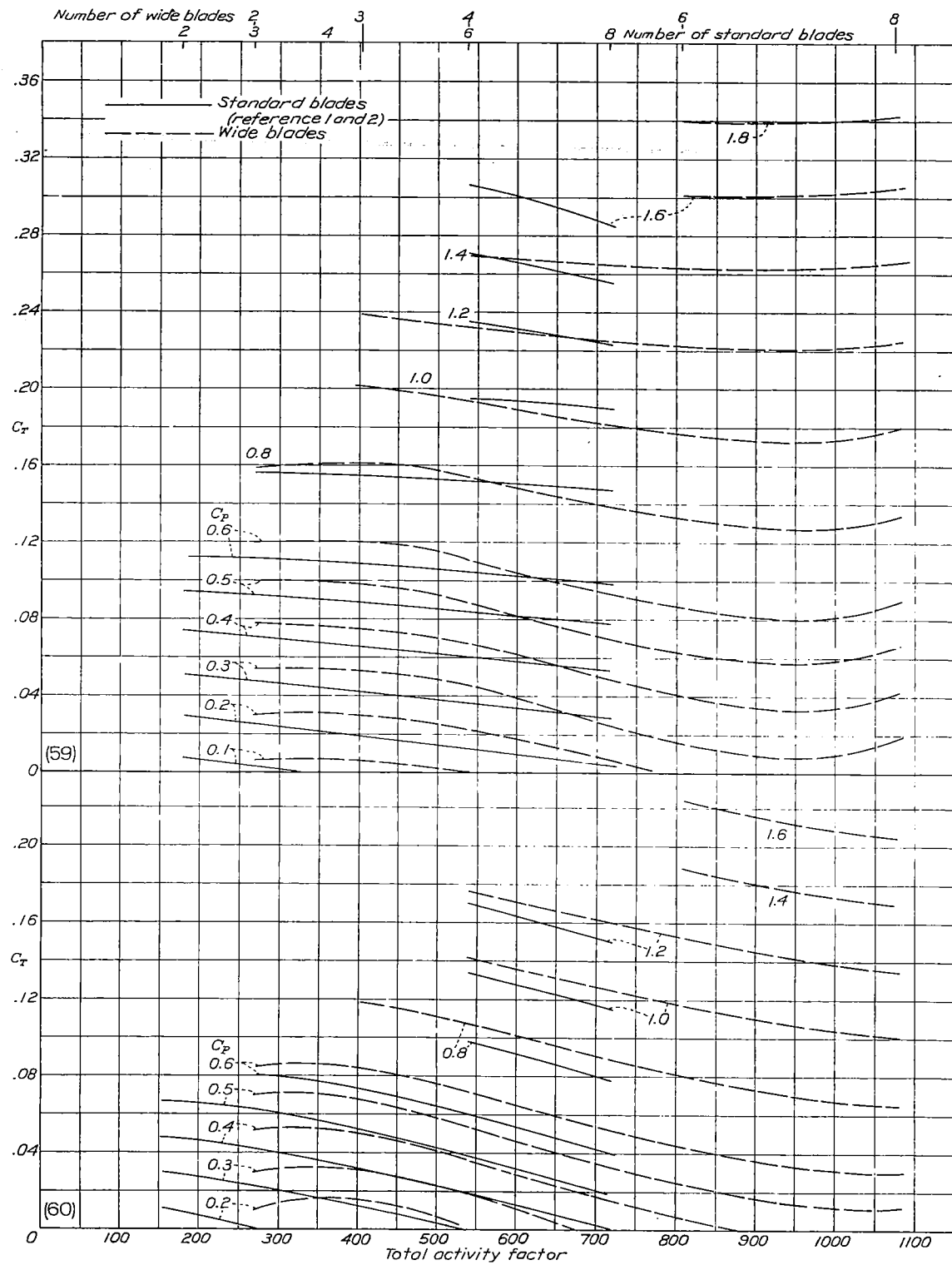


Figure 58.- Variation of thrust coefficient with activity factor.
 $V/nD = 3.0$.

(59) $V/nD = 4.0$ (60) $V/nD = 5.0$

Figures 59 and 60.- Variation of thrust coefficient with activity factor.

NACA

Fig. 61

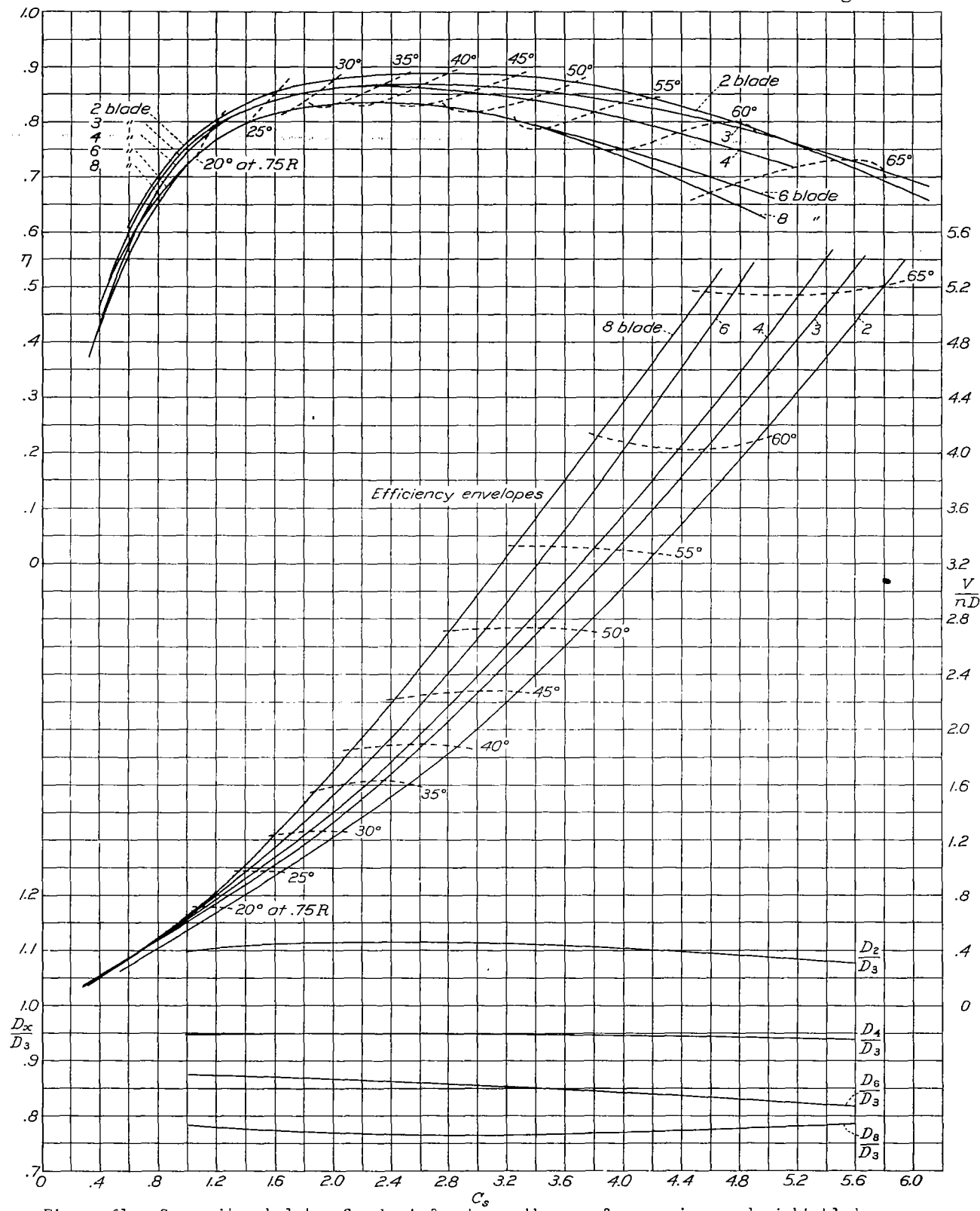


Figure 61.- Composite skeleton C_s chart for two-, three-, four-, six-, and eight-bladed; single rotation; propellers 7155-C-1.5.

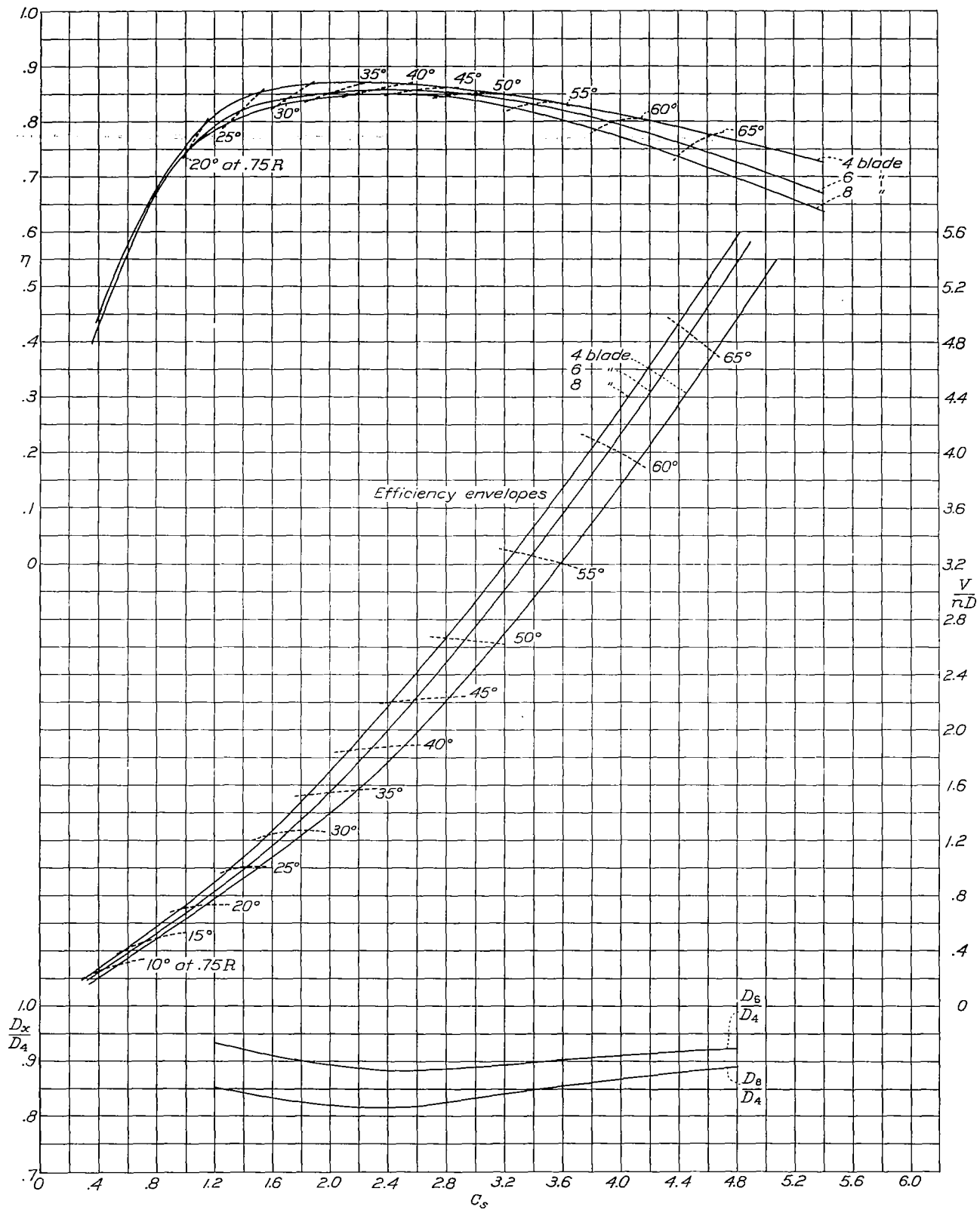


Figure 62.- Composite skeleton C_s chart for four-, six-, and eight-blades; dual rotation; propellers 3155-6-1.5 and 3156-6-1.5.

LANGLEY RESEARCH CENTER



3 1176 01354 2932